HEAT TRANSFER IN VERTICAL TUBES

WITH

COILED WIRE TURBULENCE PROMOTORS

HEAT TRANSFER IN VERTICAL TUBES

WITH

COILED WIRE TURBULENCE PROMOTORS

By

PRAMOD KUMAR, B. E.

A Thesis

Submitted To The Faculty of Graduate Studies

In Partial Fulfilment of the Requirement

for the Degree

Master of Engineering

McMaster University

November, 1968

MASTER OF ENGINEERING (1968) McMASTER UNIVERSITY
(Mechanical Engineering) Hamilton, Ontario

TITLE: HEAT TRANSFER IN VERTICAL TUBES WITH COILED WIRE TURBULENCE PROMOTORS

AUTHOR: PRAMOD KUMAR, B.E. (Indian Inst. of Tech., Delhi)

SUPERVISOR: PROFESSOR R. L. JUDD

NUMBER OF PAGES: 83

SCOPE AND CONTENTS:

An experimental study of forced convection heat transfer and friction in water flowing in a vertical tube is reported in this thesis. The study investigates the effect of coiled wire turbulence promotors of various pitch to diameter ratios (ranging from 1.00 to 5.50) upon the Nusselt Prandtl modulus $Nu/Pr^{1/3}$ and Fanning friction factor f. The investigation is carried out for three different wire sizes, 0.052 in., 0.063 in., 0.072 in. respectively.

Analysis of the various dimensionless numbers computed from the measurements of the present study indicates that the heat transfer increases by as much as 250% for low values of pitch to diameter ratio, though at the cost of a much larger increase in pressure drop. Consequently, the tubes using coiled wire turbulence promotors can be employed with advantage for cases where pumping power is not the dominating factor and reduction in weight and size of the equipment are more important.

The experimental data are empirically correlated in terms of the ratio of Nusselt numbers for the tubes with turbulence promotors to the empty tube as a function of Reynolds number and pitch to diameter ratio.

$$\frac{Nu}{Nu_o} = K(Re)^a \ (H/D)^{-0.3}$$

To evaluate the net effect of coiled wire turbulence promotors, the ratio

$$j/f = \left[\frac{Nu}{RePr^{1/3}}\right] \Big/ f$$

is plotted against Reynolds number. The curves for the coiled wire turbulence promotors fell below the theoretical curve for the empty tube indicating that coiled wire turbulence promotors are not advantageous in terms of heat transfer per unit pressure drop.

ACKNOWLEDGEMENTS

The author would like to express his appreciation to Professor R. L. Judd who provided constant assistance and support throughout the course of this experimental investigation. The author would also like to express his thanks to Mr. M. Brown and Mr. J. Crookes for their assistance in the construction of the various parts in the experimental equipment.

The financial support provided through National Research Council Grant A1585 is gratefully acknowledged.

TABLE OF CONTENTS

TEXT	PAGE NO.
1. Introduction	1
2. Literature Survey	5
3. Experimental Apparatus	10
3.1 Circulation Loop	10
3.2 Test Section	12
3.3 Test Instrumentation	13
4. Test Conditions	18
5. Test Procedure	20
6. Data Reduction	23
6.1 Evaluation of Dimensionless Numbers	23
6.2 Uncertainty Analysis	27
7. Results and Discussions	33
8. Conclusions	39
9. Nomenclature	41
10. References	43
11. Illustrations	44
APPENDIX	
A. Calibration of Orifice Plates	59
B. Effect of Various Mass Flow Rates on the Position of the Coil	61
C. Analysis of Temperature Data	63
D. Sample Calculations	68
E. Derived Results	71
F. Analysis of Heat Losses and Temperature Drop	78

LIST OF FIGURES

1. Arrangement of Various Components Comprising the Circulation Loop.

2. Test Facility

3. Test Section Assembly

4. Location of the Nine Tube Wall Thermocouples

5. Development of Tube Surface

6. Nussult Prandtl Modulus vs. Reynolds Number - Wire Diameter = 0.052 in.

7. Nussult Prandtl Modulus vs. Reynolds Number - Wire Diameter = 0.063 in.

8. Nussult Prandtl Modulus vs. Reynolds Number - Wire Diameter = 0.072 in.

9. Fanning Friction Factor vs. Reynolds Number - Wire Diameter = 0.052 in.

10. Fanning Friction Factor vs. Reynolds Number - Wire Diameter = 0.063 in.

11. Fanning Friction Factor vs. Reynolds Number - Wire Diameter = 0.072 in.

12. j/f Ratio vs. Reynolds Number - Wire Diameter = 0.052 in.

13. j/f Ratio vs. Reynolds Number - Wire Diameter = 0.063 in.

14. j/f Ratio vs. Reynolds Number - Wire Diameter = 0.072 in.

15. Empirical Correlation of Experimental Data

16. Calibration Curves for the Orifice Plates

17. Position of the Coil at Various Mass Flow Rates

18. Comparison of the Two Wire and Three Wire Thermocouples

19. Comparison of Bulk Temperatures Measured with Bulk Thermometers and Bulk Thermocouples

20. Evaluation of ΔT_f and T_f

CHAPTER 1

INTRODUCTION:

In the design of many types of heat transfer apparatus two important aspects must be considered:

(a) The rate of heat transfer which governs the size of the apparatus.

(b) The pressure drop in frictional flow which determines the pumping power.

Generally, apparatus is designed to obtain a maximum heat transfer rate with a minimum loss of energy so that equipment size is reduced advantageously. To achieve these objectives simultaneously, various methods are used, one of which is the introduction of a turbulence promotor in the heat transfer section.

Helically coiled wires and twisted tapes are two types of turbulence promotors which have been generally employed. Twisted tapes are usually fitted snugly into the tube so that the flow at the entrance is divided into two halves and spiralling is induced in the flow in each passage. This type of turbulent vortex flow can be achieved by various other methods. The first of these methods is called a vortex ramp in which the fluid is injected tangentially into a convergent duct where fluid is accelerated to achieve the required vortex strength. Due to unguided flow inside the tube, the swirl decays as the fluid flows downstream and this scheme is therefore limited to short test section lengths. The second method is called tangential injection where the vortex motion is maintained by the repeated addition of fluid through injection holes along the test section. In the third method, vortex flow is obtained by using a twisted tube of oval cross section. The introduction of a helically coiled wire in a tube produces a more complicated flow pattern which is mainly turbulent. This type of turbulence promotor approximates an integral internal fin. Helical flow is developed at the periphery of the tube superimposed upon a central core which is practically unaffected. Helical flow is induced due to a pressure gradient existing along the wire coiled inside the tube. The introduction of a coiled wire in a tube is expected

a) to produce rotational flow which would result in the generation of gravity induced currents in a single phase flow especially in the case of wall heating,

b) to introduce roughness elements which will affect the velocity distribution, the turbulence, frictional drag and reduce the boundary layer thickness.

The consequence of introducing a coiled wire into a tube is increased eddy diffusive heat and mass transfer and increased fluid friction due to increased surface area and turbulent wall shear. However, it is anticipated that at high mass flow rates, the coiled wire turbulence promotors will act as roughness elements alone and the helical flow effect would be of no consequence. Thus the heat transfer rate will tend to that of a rough empty tube.

Various experimenters have worked with both twisted tapes and coiled wires. One general conclusion derived was that twisted tapes and coiled wires with the same pitch to diameter ratio gave identical heat transfer values though a higher value of friction factor was obtained in the latter case. Manufacturing difficulties limit the minimum pitch to diameter ratio to approximately 3.0 in the case of twisted tapes, thus limiting the amount by which heat transfer can be increased. Coiled wires, on the other hand, can be manufactured with pitch to diameter ratios as low as 0.25 and are not subject to same limitations. Thus in certain cases, especially, where size of equipment is more important than power required to run it, coiled wires are a better proposition for increasing the heat transfer rate. Such cases might be:

(a) The evaporator of a vapour compression plant because pressure drop in the evaporator tube is of no consideration in this system. The total pressure drop which is normally accomplished in the throttle valve can be suitably apportioned between the throttle valve and the evaporator tube.

(b) Steam condensers in steam power plants where mechanical energy is quite cheap.

(c) Heat transfer equipment on portable units where weight and size are the main points of consideration.

The present work is conducted with the aim of evaluating the effect of helically coiled wires of various diameters (0.050 in. - 0.075 in.) and pitch to diameter ratios (1.0 - 5.5) on the heat transfer and friction characteristics of water flowing vertically in a uniformly heated circular tube 0.48 in. inside diameter for various conditions of heat flux (4780 Btu/hour - 45000 Btu/hour) and mass flow rate (10 lbs/min. - 100 lbs/min.)

CHAPTER 2

LITERATURE SURVEY:

Nagaoka and Watanabe (1) conducted experiments with coiled wire turbulence promotors. The test section consisted of a copper tube 5 1/2 feet long through which water was circulated at various mass flow rates. Water was heated by means of oil passing through an annulus surrounding the test section. The Reynolds numbers at which the work was performed, ranged from 10,000 to 50,000. It was found that increase in heat transfer per unit power loss in frictional flow was more than that in case of the empty tube.

The data of Nagaoka and Watanabe showed that the ratio of the Nusselt number for the tube with a coiled wire turbulence promotor to Nusselt number for the empty tube was a function of pitch to diameter ratio H/D only. The H/D exponent appeared to be -0.35 for the 1.06 in. I.D. tube. The ratio appeared to be independent of Reynolds number as all the curves for Nusselt number versus Reynolds number were parallel to the curve for the empty tube.

In 1957, Margolis (2) performed experiments with two tube sizes, 0.53 in. I.D. and 1.12 in. I.D. respectively and used both oil and water heated by means of steam condensing in an outer jacket surrounding the test section whose heated length was 3.67 feet. The range of Reynolds numbers extended from 10,000 to 100,000. The coiled wire turbulence promotors were made from soft steel wire

0.65 in. in diameter.

Margolis observed that an increase up to 300% could be obtained in heat transfer when water was used, but only 60% increase was obtained for air. Moreover, with both working fluids, the heat transfer increase was much less in the case of the bigger tubes. From this observation Margolis deduced that centrifugal acceleration governed the heat transfer effects of coiled wire turbulence promotors. Margolis noted the existence of a critical value of pitch to diameter ratio beyond which no appreciable increase in heat transfer was obtained.

Margolis used the ratio of Colburn j factor to the Fanning friction factor f to evaluate the performance of the various turbulence promotors investigated. It was found that with water in the 0.53 in. I.D. tube, the ratio was higher than that for the empty tube in the Reynolds number range of 40,000 to 100,000. However, ratios for air in both the 0.53 in. I.D. and 1.12 in. I.D. tubes were lower than those for the empty tube case. From this observation, Margolis concluded that a real gain in terms of increased heat transfer without comparable increase in loss of power could be achieved for certain fluids, in a limited range of Reynolds numbers, and for a limited range of tube sizes.

Using simplified equations recommended by Schneider (3), Margolis concluded that the maximum increase in heat transfer rate due to fin effect alone was of the order of 30%.

Margolis does not show any readings for the empty tube in his thesis so that it could not be ascertained whether the empty tube data was in agreement with the conventional heat transfer relation given by

$$Nu = 0.023\ Re^{0.8}\ Pr^{1/3} \qquad - \qquad (2.1)$$

Assuming Equation (2.1) to represent the data for the empty tube case, Margolis' data showed that in the 1.12 in. I.D. tube, the pitch to diameter ratio exponent was -0.3 for the case of water and -0.15 for the case of air. Furthermore, in the 0.53 in. I.D. tube the pitch to diameter ratio exponent was -0.35 for water and -0.5 for air. However, this could not be stated conclusively as Margolis used only 2 or 3 pitch to diameter ratios for each case and the data showed considerable scatter. Margolis' data indicated that the Nusselt number ratio Nu/Nu_o was not a function of Reynolds number showing that the percentage increase in heat transfer was the same for all values of Reynolds number.

Later Kreith and Margolis (4) reanalysed the same data and stated that the experimental data for the empty tube was within $\pm 15\%$ of Equation (2.1). They plotted the ratio Nu/Nu_o against Reynolds number and the plots indicated that for the 1.12 in. I.D. tube the ratio was independent of Reynolds number for both air and water. However, in the 0.53 in. I.D. tube with water, the Reynolds number exponent was found to be 0.23.

Bhatia, Kumar, and Sud (5,6) conducted experiments with both coiled wire and twisted tapes fitted inside a 13/16 in. I.D. copper tube, 42 in. long. Dry compressed air was heated by means of steam condensing in an outer jacket at a pressure of 2.2 $Kg./cm^2$

absolute. The Reynolds numbers investigated ranged from 7000 to 60,000. Coiled wire turbulence promotors were made from spring brass wire 0.040 in. diameter.

The Fanning friction factor values were not quite in agreement with the trend observed by Kreith and Margolis. Friction factors in the present study were found to first decrease and then increase with increasing Reynolds Numbers, whereas friction factors in the Kreith and Margolis study (3,4) monotonically decreased with increasing Reynolds numbers. The critical Reynolds number at which the inflection occurred was found to decrease for decreasing pitch to diameter ratios. The discrepancy was explained on the basis of perceptible zones of flow separation existing downstream of wire. (Figure - 8 of Reference 12). At low values of Reynolds number, the eddy formed downstream of wire at a particular location did not extend to the next location. However, as the Reynolds number increased or the pitch decreased, the eddy extended to the next location resulting in a zone of flow separation.

Curves were drawn to optimize the effects of coiled wires in the heat transfer and power loss characteristics from which the authors concluded that a critical value of minimum pitch to diameter ratio existed. Pitch to diameter ratios from 0.550 to 0.325 gave approximately the same values of Nusselt number, though the friction factors increased considerably. From this observation, the authors concluded that it was not advantageous to use coiled wires with pitch to diameter ratios less than 0.6. Pitch to diameter ratios from 1.5 to 3.5 were found to give optimum results; a fairly large increase in heat transfer and a reasonable increase in pumping power. The heat transfer data of Bhatia and Kumar indicated that the $\frac{Nu}{Nu_o}$ was proportional to $(H/D)^{-0.2}$. However, the Nu/Nu_o ratio was found to be independent of Reynolds number.

CHAPTER 3

EXPERIMENTAL APPARATUS

The various components comprising the test apparatus were arranged to form a closed loop. Water was circulated through a gear pump section, an electrical heater section, a flow measuring section, the test section, and a cooler section. The arrangement of the various components is shown schematically in Figure 1. Figure 2 shows a photograph of the test apparatus.

3.1 Circulation Loop

A detailed description of the circulation loop is given in Chapter 3.1 of Reference (7).

A Worthington model 6GBU rotary pump geared to an electric motor discharged water at a constant rate of 55 U.S. gallons/minute at any pressure level upto 50 pounds per square inch. A portion of the mass flow in excess of that required for a particular test was recirculated through the pump by means of an external bypass. The mass flow selected then passed through a heater section whose output could be varied continuously from 0 - 12000 watts. The heat source was a Chromalox model TM612 flanged pipe heater comprised of six Calrod elements.

To cover a fairly large range of Reynolds numbers and to obtain reasonable accuracy, the flow meter section was comprised of two orifice plates in different pipes 1.5 in. I.D. and 1.0 in. I.D. respectively arranged parallel to each other and valved so that either one could be used independently. The orifice plates were designed in accordance with the British Standard Code (BS1042:A43) and calibrated by passing water through the orifices and collecting it in a tank. The corresponding differential pressure drop was measured by a mercury differential manometer and the mass flow collected in the tank was determined by weighing. Calibration curves for the two orifice plates are shown in Appendix A . The flow meter section described was capable of measuring a range of flow rates requiring a pressure differential varying in magnitude from 1 in. of mercury to 36 in. of mercury. The orifice plate in the 1.0 in. I.D. pipe measured flows from 0.82 lbs./minute (1 in. Hg.) to 49 lbs./minute (35 in. Hg.) and the orifice plate in the 1.5 in. I.D. pipe measured flows from 30 lbs./minute (1 in. Hg.) to 161 lbs./minute (35 in. Hg.).

Heat was removed from the water by passing it through a cooler section comprised of a Heliflow model 9XF-16S heat exchanger in which heat was exchanged with cold water from the mains. Fine control of the main water was achieved by means of a small valve upstream of the cooler section.

A 5 U.S. gallon capacity head tank was connected upstream of test section to accomodate expansion of water. The head tank was mounted higher than any other point in the system to keep it flooded during operation. The head tank was vented on top to establish atmospheric conditions upstream of the gear pump section.

3.2 Test Section

Figure 3 illustrates the test section assembly. The test section consisted of a thin stainless steel tube 0.5 in. O.D. and 0.01in. W.T. by 34 in. long . The heated length of the tube was only 24 in. since two copper lugs which served as electrical connectors were silver soldered on the tube 24 in. apart, 5 in. from each end of stainless steel tube. Three pressure tappings were provided in the tube at each copper lug separated by 120 degrees, so that three independent measurements of the differential pressure drop across the test section could be made for averaging purposes. The test section was connected to the circulation loop by means of two stainless steel housings, one at each end. The ends of the test section extended into the housings through O-ring seals provided to permit expansion and prevent leakage.

The power supply for the test section was a Miller model SR1000 B1 D.C. welding transformer. The heat generation in the test section could be regulated by a control knob provided with the machine enabling a continuous variation from 1 K.W. to any desired value upto 15 K.W.

The coiled wire turbulence promotors were manufactured from spring brass wire 0.034 in. in diameter and 0.042 in. in diameter covered with either teflon 'thin wall' spaghetti tubing or Illumitronic vinyl sleeving to give 3 effective wire sizes, 0.052 in., 0.063 in., and 0.072 in. in diameter respectively. Initial experiments were performed in which a plexiglass tube 5/8 in. O.D. and 1/2 in. I.D. was fitted in place of the test section with wire coils inserted to evaluate the effect of high mass flow rates on the position of the wire coils. It was observed that the coils were under sufficient tension to hold themselves against the tube wall under all flow conditions. Appendix B shows some photographs of the wire coil under various conditions of mass flow rate .

3.3 Test Instrumentation

The various temperatures in the test section were measured with eleven chromel - constantan thermocouples. One thermocouple was immersed in the water upstream of the test section; nine thermocouples were spotwelded on the outside of the heated tube; and one thermocouple was immersed in the water downstream of test section. The nine thermocouples spotwelded on the outside of the test section were positioned along the length of the tube in two diametrically opposite groups 5 in. apart. These two groups were comprised of four "two wire thermocouples" and five "three wire thermocouples" respectively. Figure 4 shows the location of the nine tube wall thermocouples.

Because of the direct current heating used in this study, it was essential to find a way of preventing the thermocouples from "picking up" voltage from the tube which would mask the thermoelectric potential. After a series of trials, it was found that the following method solved the problem satisfactorily:

For the two wire thermocouples, a 30 gauge chromel wire was spotwelded on the tube at the specified location. The underside of the wire was insulated from the tube by means of fiberglass insulation tape and then a 36 gauge constantan wire was spotwelded on the chromel wire approximately 0.01 in. from the junction. After using this technique for spotwelding the thermocouples, it was found that the thermocouples still picked up very small amounts of voltage (ranging from 0.010 - 0.15 mv.) from the tube. This was corrected by calibrating the thermocouples "in situ" prior to the commencement of the tests. Readings were taken at a particular steady state condition for both normal and reverse welding transformer polarity. The difference of the two readings for each of the various thermocouples yielded twice the correction required. The maximum correction for the two wire thermocouples was found to be of the order of 0.15 mv. corresponding to the maximum value of heat dissipation.

The three wire thermocouples consisted of two 30 gauge chromel wires and one 30 gauge constantan wire spotwelded to the tube 1/8 in. apart around the circumference. The constantan wire was spotwelded in between the two chromel wires and the three junctions were spaced approximately 0.01 in. apart longitudinally. The two chromel wires were then led to a board and connected to the ends of 36 gauge bare chromel wire 40 in. long. A wiper which moved along the 36 gauge wire was so located that the voltage picked off exactly equalled the voltage level of the constantan wire. The initial balance of the three wire thermocouples was achieved by applying a small D.C. voltage (0.5 volts) to the electrical connectors and noting the initial response of the three wire thermocouple by means of a potentiometer before the heating effects set in. The final balance was obtained by applying the heating voltage and reversing the polarity of the welding transformer a number of times. The three wire thermocouples were calibrated prior to the tests to provide corrections for the small unbalance which remained, using the same procedure as with the two wire thermocouples.

To ensure against undetected changes in the thermocouple calibration, all thermocouples were calibrated six times during the course of experimentation. Every fourth test run was taken in the manner of the calibration test run by reversing the polarity of the welding transformer. Figure 18 in Appendix C compares the wall temperatures measured with these two types of thermocouples.

Initially the two stream thermocouples were formed from Thermoelectric "Ceramo" miniature sheathed thermocouple wire with inert oxide insulation. The chromel constantan pair contained by the sheath was welded together and grounded to the sheath at the hot junction. It was found that the temperatures read by these thermocouples in the presence of D.C. heating were not correct in as much as the temperatures read by the precision mercury in glass thermometers and the thermocouples differed in magnitude by 2°F.

or more depending upon the heating voltage. Moreover, these thermocouples corroded after a few tests. In an attempt to correct this deficiency, thermocouples were made from 36 gauge nylon insulated chromel-constantan thermocouple wire inserted in a 0.040 in. I.D. stainless steel tube. The junction was insulated from the stainless steel sheath by means of a plug of epoxy. This procedure, also, proved somewhat unsatisfactory as the thermocouples were still influenced by the D.C. heating but to a much lesser extent. However, the effect upon the upstream and downstream thermocouples was found to be the same with respect to magnitude and polarity and the temperature difference corresponded to the bulk temperature difference as indicated by the mercury in glass thermometer within $\pm$ 5%. Finally, it was decided to use the precision mercury in glass thermometers installed in thermometer wells located upstream and downstream of test section for measuring bulk temperatures. The thermometers measured temperatures with sufficient accuracy as evidenced by the fact that the heat flux calculated from calormetric measurements agreed well with the heat flux calculated electrically. Figure 19 in Appendix C compares the bulk temperatures measured by bulk thermocouples and bulk thermometers in a typical test.

The thermoelectric potential of the eleven thermocouples were recorded on a Philips model PR 3210 A/00 twelve point self balancing millivolt recorder. Thermoelectric potentials of the therm-ocouple upstream of the test section and the nine thermocouples were referenced to an ice junction, whereas, the thermoelectric potential of the bulk thermocouple downstream of test section was referenced to the bulk thermocouple upstream of test section to give the bulk temperature rise directly.

The heat generated in the test section was calculated from measurements of potential drop over the test section. A Conway model No. 655780 variable range voltmeter with $\pm$ 1% full scale accuracy measured the potential drop over the test section and a Simpson model 29SC-No-10028 ammeter with $\pm$1% full scale accuracy measured the current flowing through the test section when used in connection with a shunt.

The pressure drops over the test section, and the differential pressures induced by the flow through the orifice plates were measured by means of five 36 in. differential mercury manometers Meriam model No - 10 AA25WM with an uncertainty in the measurement no greater than ($\pm$ 5%).

CHAPTER 4

TEST CONDITIONS

This chapter outlines the various mass flow rate, temperature and heat flux conditions used in this study.

The water mass flow rate was varied from 10 lbs/minute to 120 lbs/minute incrementally resulting in nine sets of readings for each test run corresponding to a particular pitch to diameter ratio and wire size. However, for low values of pitch to diameter ratio of the order of 1.00, the mass flow rate was limited to a maximum of approximately 50 lbs/minute. The range of mass flow rates described above, in conjunction with the temperature conditions used in this study, yielded Reynolds numbers ranging from a minimum of 7,000 to a maximum of 150,000.

Inlet water temperature was maintained within plus or minus 5 degrees of room temperature. Accordingly, during the course of the test run the temperature of the water ranged from 80°F to 90°F. The heat dissipation was adjusted for each test to yield a bulk temperature rise of the order of 5°F to 10°F. This fairly high rise in bulk temperature minimised the error in the results associated with computing the differences of the measurements of the bulk liquid thermometers. The wall temperature for these bulk temperature conditions and mass flow rates, was observed to be approximately 15°F to 30°F higher than the bulk temperature for all the test runs using coiled wire turbulence promotors and between 30°F and 45°F higher than the bulk temperature for the case of the empty tube. Heat flux for the conditions described above, varied from 1.4 K. Watts (4780 BTU/hour) for the minimum mass flow rate of 10 lbs/minute to a maximum of 13.2 K. Watts (45,000 BTU/hour) for the maximum mass flow rate of 120 lbs./minute in the case of empty tube.

CHAPTER 5

TEST PROCEDURE

Prior to each test run, the system was filled with fresh water from the mains. The plug on top of the housing downstream of the test section was removed and air was allowed to escape while the system was filling till the housing was full of water. The plug was replaced and the remainder of the air in the system was removed in the manner described below.

The purge valves provided respectively in the housing upstream of test section and the casing surrounding the system heater were opened and the air entrapped at these locations was allowed to escape. The pump was started and the bypass valve was set for minimum mass flow rate. Fresh water was supplied to the tank while the discharge valve provided at the lowest point in the circulation loop was opened, permitting a continuous flow of water through the system. After about five minutes, the discharge valve was closed and the head tank was allowed to fill up. The mass flow rate through the system was increased to its maximum value after which the air entrained in the water was found to collect in the housing upstream of test section, where it was bled off through the purge valve. The system heater was energised and cold water was passed through the cooler section in order to maintain the bulk temperature approximately constant. Any air dissolved in the water was found to collect beneath the purge valve in the heater section and was bled off from time to time.

After about ten minutes, the mass flow rate was again adjusted to its minimum value and then the pump was shut off. Purge valves on top of the five manometers were opened and water was allowed to discharge till no air was left in the lines and the manometers indicated zero pressure differential.

The system heater was not used during the actual test runs. Initially, the minimum mass flow rate was established, an arbitrary cooling water flow rate was set and heat flux was adjusted to its minimum value. Experience enabled the rough setting of the cooling water flowrate corresponding to various heat flux conditions to be predetermined. Final adjustments, bringing the temperature of water in the system to equilibrium were made by adjusting the mass flow rate of cooling water by means of a fine control valve upstream of the cooler section.

When the various temperatures in the system had attained the values desired, five minutes were allowed to elapse in which it was ensured that steady state heat transfer conditions existed in the test section as evidenced by the fact that inlet water temperature and surface temperatures remained invariant with time. Then the following measurements were made with the appropriate instruments and recorded.

1. Flow rate of water circulating through the system
2. Pressure differences over the test section
3. Potential drop over the test section
4. Current flowing through the test section
5. Stream temperatures as indicated by the two bulk thermometers
6. Temperature of water upstream of the test section as indicated by the stream thermocouple
7. Surface temperatures at various locations on the stainless steel tube
8. Bulk temperature difference as indicated by the difference of the bulk thermocouple downstream of the test section and the bulk thermocouple upstream of the test section

The mass flow rate of water circulating through the system was increased and the corresponding heating voltage and cooling water flow rate were adjusted. This procedure was repeated to obtain the nine sets of readings comprising one test run.

Immediately after the test run, water was discharged from the system to prevent further corrosion of the bulk thermocouples. It was generally found that the plexiglass components of the housings were coated with an electrically conducting deposit which was thought to result from the deposition of impurities present in the mains water. This deposit tended to ground the wall thermocouples to the system and to circumvent this, the plexiglass components were cleaned after every two or three test runs.

CHAPTER 6

DATA REDUCTION

6.1 Evaluation of Dimensionless Numbers

All the measurements obtained during the test runs were reduced to dimensionless numbers which are tabulated in Appendix E. The following section outlines the manner in which the dimensionless numbers were computed.

The mass flow rates were read from the calibration curves for the two orifice plates (Appendix A) for the measured pressure differentials. The surface temperatures were read from "Chromel-Constantan" thermocouple conversion tables prepared by the Heat Transfer Laboratory at the University of Michigan from data published by the National Bureau of Standards (8) after correcting for the voltage pick up.

The surface temperatures were plotted on linear coordinates as a function of the distance from the upstream section of the tube to the downsteam section of the tube. The bulk temperatures were superimposed on the same plot, enabling the mean film temperature T_f and the film temperature drop ΔT_f to be evaluated. The two quantities were read from the plot about 16 inches from the upstream section of the tube where the rate of surface temperature rise with distance was approximately the same as the rate of bulk temperature rise. Since the thermocouples were spotwelded on the outside of the tube, the temperature drop in the wall estimated in accordance with Appendix F was subtracted from the temperature values determined from the plot. A typical plot used to evaluate ΔT_f

and T_f is shown in Figure 20 in Appendix C. The following procedure was used to evaluate the various dimensionless numbers.

(a) Area of Flow

Due to the presence of the coiled wire in the test section, the effective flow area was less than that for the case of an empty tube. For a particular value of H/D, the wire could be assumed to have a elliptical shape at every cross section of the tube Figure 5 represents a model formulated to take into consideration these elliptical effects. The major and minor diameter of the ellipse are calculated as follows:

Geometric considerations give $$\cos\Theta = \frac{(H/D)}{\sqrt{(H/D)^2 + \pi^2}} \tag{6.1}$$

The major diameter $$a = \frac{d}{\cos\Theta} \tag{6.2}$$

The minor diameter $b = d$

Area of flow $$A = \frac{\pi}{4}(D^2 - ab) \tag{6.3}$$

(b) Hydraulic Diameter

$$D_H = 4 \times \frac{\text{Cross Sectional Flow Area}}{\text{Wetted Perimeter}}$$

Wetted Perimeter $$P = \pi D + \pi\sqrt{\frac{a^2 + b^2}{2}} \tag{6.4}$$

Consequently $$D_H = \frac{4 \times \frac{\pi}{4}(D^2 - ab)}{\pi D + \pi\sqrt{\frac{a^2 + b^2}{2}}}$$

or

$$D_H = \frac{D^2 - ab}{D + \sqrt{\frac{a^2 + b^2}{2}}} \tag{6.5}$$

(c) Reynolds Number

$$Re = \frac{\rho V D_H}{\mu_f}$$

The product ρV was calculated by dividing mass flow rate by area of flow so that

$$Re = \frac{\dot{m}}{A} \times \frac{D_H}{\mu_f} \tag{6.6}$$

(d) Film Heat Transfer Coefficient

The film heat transfer coefficient was calculated by the following relationship

$$h_c = \frac{(\dot{Q}/A_S)}{(T_S - T_B)} = \frac{(Q/A_S)}{\Delta T_f} \tag{6.7}$$

The heat flux (Q/A_S) was computed from electrical measurements of heat generation in the tube and/or calorimeteric measurements of heat addition to water circulating through the test section.

The heat flux calculated from electrical measurements was computed by the relationship

$$(Q/A_S) = 3.413 \frac{EI}{A_S} \tag{6.8}$$

The heat flux calculated from calorimetric measurements was computed by the relationship

$$(Q/A_S) = \frac{m\ C_p\ (T_o - T_i)}{A_S} = \frac{m\ C_p\ \Delta T_B}{A_S} \tag{6.9}$$

The two independent computations of heat flux served to check the validity of the measurements of heat flux.

(e) Nussult Prandtl Modulus

In as much as the bulk fluid temperature was maintained approximately constant during the investigation, the Prandtl number variation was very slight. Consequently, the Prandtl number influence could not be evaluated and it was assumed that the Prandtl number exponent was equivalent to one third. Accordingly $Nu/Pr^{1/3}$ values were computed by the relationship

$$\frac{Nu}{Pr^{1/3}} = \frac{\frac{h_c\ D_H}{K_f}}{Pr^{1/3}} \tag{6.10}$$

where the Prandtl number was evaluated at the film temperature.

(f) Colburn j Factors

The Colburn j factors were computed by dividing the $Nu/Pr^{1/3}$ values by the corresponding Reynolds number values according to the relationship

$$j = \frac{Nu}{Re\ \ Pr^{1/3}} \tag{6.11}$$

(g) Fanning Friction Factors

The Fanning friction factors were evaluated using the relationship

$$\Delta p = 4f \frac{L}{D_H} \frac{V^2}{2g} \tag{6.12}$$

(h) j/f Ratio

Finally the j/f ratio was computed to evaluate the net effect of turbulence generators on heat transfer relative to the friction head loss.

In order to clarify the computation procedures used, sample calculations are presented in Appendix D.

6.2 Uncertainty Analysis

In performing the uncertainty analysis, the following relationship was used for each individual result computed

$$\frac{W_R}{R} = \left[\left(\frac{\partial R}{\partial V_1} \frac{W_1}{R}\right)^2 + \left(\frac{\partial R}{\partial V_2} \frac{W_2}{R}\right)^2 + \dots . \left(\frac{\partial R}{\partial V_n} \frac{W_n}{R}\right)^2\right]^{1/2} \tag{6.13}$$

where R - result

W_R - uncertainty in result

V - variable

W_n - uncertainty in nth variable

The uncertainty in the computed results indicated by this relationship represents the root mean square uncertainty resulting from the statistical combination of maximum values of individual uncertainties.

The results of uncertainty analysis are presented in a tabular form in the following pages. The uncertainty associated with reading of various fluid properties from tables and charts was disregarded.

The results of uncertainty analysis indicate that uncertainty in the correlation of heat transfer results could be as great as 8.8% and that the uncertainty in the correlation of fluid friction results could be as great as 16.5%. The uncertainty in the correlation of j/f results is even larger and can be as great as 18.7%.

UNCERTAINTY DESCRIPTION	UNCERTAINTY	COMMENTS
MASS FLOW RATE		
$m = K\sqrt{\Delta p}$		
Uncertainty in smallest weight measured during calibration (10 lbs.)	$\pm$0.25 lbs.	
Uncertainty in smallest measurement of pressure differential during calibration (1" Hg)	$\pm$0.05" Hg.	
Uncertainty in K for single point evaluation	$\pm$5.6%	Equation (6.13)
Uncertainty in K for twelve point evaluation	$\pm$1.6%	$\frac{1}{\sqrt{12}}$ x 5.6%
Uncertainty in smallest measurement of pressure differential during actual experimentation (1" Hg.)	$\pm$0.05" Hg.	
Uncertainty in mass flow rate	5.3%	Equation (6.13)
BULK TEMPERATURE DIFFERENCE		
$\Delta T_B = T_o - T_i$		
Uncertainty in smallest measurement of bulk temperature difference (4.6°F)	$\pm$0.2°F	
Uncertainty in bulk temperature difference	$\pm$4.3%	Equation (6.13)
SURFACE AREA		
$A_S = \pi DL$		
Uncertainty in D (0.480 in.)	$\pm$0.002 in.	
Uncertainty in L (24.0 in.)	$\pm$0.1 in.	
Uncertainty in surface area	$\pm$0.6%	Equation (6.13)

UNCERTAINTY DESCRIPTION	UNCERTAINTY	COMMENTS
FILM TEMPERATURE DROP		
$\Delta T_f = T_W - T_B$		
Reading uncertainty in smallest measurement of recorder (2.00 mv)	0.01 mv	
Uncertainty due to emf pick up	0.05 mv	
Uncertainty in film temperature drop	5.0%	Equation (6.13)
HYDRAULIC DIAMETER		
$D_H = \dfrac{D^2 - ab}{\sqrt{D + \dfrac{a^2+b^2}{2}}}$		
Uncertainty in wire size	$\pm$0.001 in.	
Uncertainty in hydraulic diameter	$\pm$1.9%	Equation (6.13)
HEAT FLUX		
$\dfrac{Q}{A_S} = \dfrac{3.413\ EI}{A_S}$		
Instrument uncertainty of voltmeter	$\pm$1%	Manufacturer's Rating
Reading uncertainty in smallest measurement of voltmeter (8.0 volts)	$\pm$0.2 volts	
Instrument uncertainty of ammeter	$\pm$1%	Manufacturer's Rating
Reading uncertainty in smallest measurement of ammeter (175 amps)	$\pm$2 amps	
Uncertainty in heat flux	$\pm$3.1%	Equation (6.13)
VELOCITY		
$V = \dfrac{m}{\rho A}$		
$A = \dfrac{\pi}{4}\left[D^2 - \dfrac{d^2}{\cos\theta}\right]$		
Uncertainty of area of flow	$\pm$2.8%	Equation (6.13)
Uncertainty in Velocity	$\pm$6.0%	Equation (6.13)

UNCERTAINTY DESCRIPTION	UNCERTAINTY	COMMENTS
FILM HEAT TRANSFER COEFFICIENT $h_c = \frac{Q}{A_S \, \Delta T_f}$		
Uncertainty in film heat transfer coefficient	$\pm$ 5.9%	Equation (6.13)
REYNOLDS NUMBER $Re = \frac{\rho V D_H}{\mu_f}$		
Uncertainty in Reynolds number	$\pm$6.3%	Equation (6.13)
NUSSELT PRANDTL MODULUS $\frac{Nu}{Pr^{1/3}} = \frac{h_c \; D_H}{K_f \; Pr^{1/3}}$		
Uncertainty in Nusselt Prandtl modulus	$\pm$6.2%	Equation (6.13)
FANNING FRICTION FACTOR $f = \frac{2g}{4} \frac{D_H}{L} \frac{\Delta p}{V^2}$		
Uncertainty in smallest measurement of Δp (0.4" Hg)	$\pm$0.05" Hg.	
Uncertainty in friction factor	$\pm$15.2%	Equation (6.13)
COLBURN j FACTOR $j = \frac{Nu}{RePr^{1/3}}$		
Uncertainty in j	8.8%	Equation (6.13)

UNCERTAINTY DESCRIPTION	UNCERTAINTY	COMMENTS
j/f RATIO		
Uncertainty in j/f ratio	17.6%	Equation (6.13)

Uncertainty in correlating heat transfer results as computed by equation (6.13) ∿ 8.8%

Uncertainty in correlating friction factor results as computed by equation (6.13) ∿ 16.5%

Uncertainty in correlating j/f results as computed by equation (6.13) ∿ 18.7%

CHAPTER 7

RESULTS AND DISCUSSIONS

The data for the empty tube was found to correlate within $\pm 10\%$ with the Colburn heat transfer relationship (9) given by:

$$\frac{Nu}{Pr^{1/3}} = 0.023\ Re^{0.8} \tag{7.1}$$

in which the property values of the fluid were evaluated at the film temperature.

The friction factor data correlated within $\pm 15\%$ for low Reynolds numbers and within $\pm 5\%$ for high Reynolds numbers with the von Kármán's relationship for a smooth tube (10) given by

$$\sqrt{\frac{4}{f}} = 2\log_{10}\left(Re\sqrt{f/4}\right) - 0.8 \tag{7.2}$$

which is approximated by the relationship

$$f = 0.046\ Re^{-0.2} \tag{7.3}$$

This approximate relationship in combination with the Colburn heat transfer relationship gave

$$j/f = 0.5 \tag{7.4}$$

as the theoretical value for the empty tube. The j/f ratio computed from the same data for the empty tube was found to correlate within $\pm 10\%$ of the value predicted by Equation (7.4) for the empty tube. This agreement with the predictions for an empty tube established confidence in the measuring technique.

Figures (6 - 8) show plots of $Nu/Pr^{1/3}$ versus Re for the three wire sizes used. These curves clearly indicate that decreasing the pitch to diameter ratio at constant Reynolds number increases the heat transfer. Moreover, it is noticed that the heat transfer increase is inversely proportional to Reynolds number at constant pitch to diameter ratio. The maximum increase in heat transfer obtained is of the order of 250% corresponding to pitch to diameter ratios of the order of 1.00.

Figures (9 - 11) show the variation of Fanning friction factor with Reynolds number for the three wire sizes used. It is observed that friction factors increase with decreasing pitch to diameter ratios at constant Reynolds number and decrease with increasing Reynolds number at constant pitch to diameter ratio.

Figures (12- 14) indicate the variation of j/f with Reynolds number for the three wire sizes used. It is seen that j/f ratio decreases with increasing Reynolds number for a constant value of pitch to diameter ratio. This is contrary to Kreith's finding that the j/f ratio increased with increasing Reynolds number. Moreover, the curves for the various turbulence promotors all lie below the curve for the empty tube except for the curve corresponding to the 0.052 in. diameter wire and then only for the largest pitch to diameter value investigated and only below a Reynolds number value of 15,000. The implication of this observation is that although it is possible to increase heat transfer by the use of turbulence promotors, the corresponding friction head loss increases even more so that in general, the empty tube always offers the greatest heat transfer per unit friction head loss. This finding is again contrary to that of Kreith and Margolis who found that it was possible to improve upon the empty tube for certain values of Reynolds number and pitch to diameter ratio. The explanation of this discrepancy is not known, but it is noteworthy that surface temperature was maintained constant in Kreith's investigation whereas the surface heat flux was maintained constant in the present investigation. Moreover, the turbulence promotors used in the present investigation were insulated and did not act as fins whereas in Kreith's investigation, wire coils were not insulated from the heat transfer surface and thus tended to act as integral fins.

An empirical correlation of the form

$$\frac{Nu}{Nu_o} = K\, Re^{a}\left(\frac{H}{D}\right)^{-0.3} \qquad (7.5)$$

was fitted to the experimental data by crossplotting the ratio of Nusselt number for tubes with coiled wire turbulence promotors to the Nusselt number for the empty tube first as a function of H/D at four different values of Reynolds number and then as a function of Reynolds number at constant H/D ratio. It was found that 85%

of the data points fell within $\pm 10\%$ of the fitted equation. Figure (15) shows the correlation of Nu/Nu_o with $k(Re)^a(H/D)^{-0.3}$; Table I below indicates the numerical values obtained for the parameters k and a. The H/D exponent was found to be -0.3 for the three wire sizes used and from this observation it can be concluded that the H/D index is independent of wire size. However, the Reynolds number exponent was found to decrease with increasing wire size. It appears that the Reynolds number exponent varies linearily with wire size, although it is not possible to state this conclusively.

TABLE I

TABULATION OF PARAMETERS

(d/D)	k	a
.108	7.5	-.11
.131	9.0	-.13
.150	12.0	-.15

It was indicated by Kreith and Margolis (4) that the heat transfer for tubes with coiled wire turbulence promotors was dependent upon the centrifugal force. Furthermore, there was a considerable difference in heat transfer increase for the two fluids, water and air. In as much as the heat transfer increase with coiled wire turbulence promotors is dependent upon the centrifugal force and the density of the fluid, it will not be worthwhile comparing the data of the present study with Kreith and Margolis' data for the 1.12 in. I.D. tube and for air. However, Kreith and Margolis used a 0.53 in. I.D. tube so that it is reasonable to evaluate the agreement of the two sets of data for water with coiled wire turbulence promotors of 0.065 in. diameter.

The data by Kreith and Margolis (4) indicated that the Reynolds number exponent was 0.23, whereas in the present case, the Reynolds number exponent was found to be -0.135. The reason for this discrepancy is not known but this variation of heat transfer indicates that as the Reynolds number increases, the heat transfer increase decreases. The implication of this observation might be that at high Reynolds numbers, the coiled wire turbulence promotors no longer produced any helical flow and tended to act as random roughness elements. Thus the heat transfer tended to approach the heat transfer for the case of a rough empty tube.

Kreith and Margolis' data indicated that the H/D exponent approximated -0.35 whereas in the present investigation the H/D exponent was found to be -0.3. This agreement is felt to be quite significant.

Table II below shows the various values of H/D exponent and Reynolds number exponent for various tube sizes and for air and water, fitted to the equation

$$\frac{Nu}{Nu_o} = k\, Re^a (H/D)^b$$

as found by various authors.

TABLE II

COMPARISON OF H/D EXPONENT AND REYNOLDS NUMBER EXPONENT

Wire Diameter	Tube Diameter	Fluid	H/D Exponent	Re Exponent	Author(s)
---------	1.06 in.	Water	-0.35	Zero	Nagaoka and Watanabe (1)
0.065 in.	0.53 in.	Water	-0.35	Zero	Margolis (2)
0.065 in.	0.53 in.	Air	-0.50	Zero	Margolis (2)
0.065 in.	1.12 in.	Water	-0.3	Zero	Margolis (2)
0.065 in.	1.12 in.	Air	-0.15	Zero	Margolis (2)
0.065 in.	0.53 in.	Water	-0.35	0.23	Kreith and Margolis (4)
0.040 in.	13/16 in.	Air	-0.20	Zero	Bhatia & Kumar (5)
0.052 in.	0.48 in.	Water	-0.30	-.110	Present work
0.063 in.	0.48 in.	Water	-0.30	-.130	Present work
0.072 in.	0.48 in.	Water	-0.30	-.150	Present work

CHAPTER 8

CONCLUSIONS

This study presents a comprehensive set of measurements evaluating the effect of coiled wire turbulence promotors on the friction and heat transfer characteristics inside circular tubes under various conditions of flow rate and heat flux. Three different wire sizes 0.052 in., 0.063 in., 0.072 in. respectively were used to evaluate the effect of wire diameter which had been largely ignored by other research workers.

The results of the present study indicate that coiled wire turbulence promotors are less effective than an empty tube in terms of heat transfer per unit pumping power. It was observed that the heat transfer could be increased considerably, of the order of 250%, but the loss due to increased friction was much greater than the gain due to increased heat transfer. However, coiled wire turbulence promotors can be effectively used where pumping power is of little importance and reduction in size and weight of the equipment are the dominating factors.

An empirical correlation of the form

$$\frac{Nu}{Nu_o} = k\ Re^a\ (H/D)^{-0.3}$$

was fitted to the experimental data relating the heat transfer for the tubes using coiled wire turbulence promotors to that for the empty tube as a function of Reynolds number and H/D ratio.

This empirical equation can be used for preliminary design purposes in designing heat exchangers using coiled wire type of turbulence promotors.

NOMENCLATURE

Arabic Symbols	Description	Units
A	Flow Area	Ft^2
A_S	Surface Area	Ft^2
a	Major Diameter Of Ellipse	Ft
b	Minor Diameter Of Ellipse	Ft
C_p	Specific Heat	BTU/lb°F
D	Diameter	Ft
d	Wire Diameter	Ft
D_H	Hydraulic Diameter	Ft
E	Potential Drop Over The Test Section	Volts
f	Fanning Friction Factor	
g	Gravitational Acceleration Constant	ft/hr^2
h_c	Film Heat Transfer Coefficient	$BTU/hr.ft^2 °F$
I	Current Flowing Through Test Section	Amperes
j	Colburn j Factor	
K_f	Thermal Conductivity At Film Temperature	BTU/hr. Ft°F
L	Effective Length	Ft
m	Mass Flow Rate	lbs/hr
Δp	Pressure Drop Over The Test Section	Ft of water
Q	Heat Generation	BTU/hr
T	Temperature	°F
T_B	Bulk Temperature	°F
ΔT_B	Bulk Temperature Rise	°F

T_f	Film Temperature	°F
ΔT_f	Film Temperature Drop	°F
T_i	Inlet Bulk Temperature	°F
T_o	Outlet Bulk Temperature	°F
T_W	Wall Temperature	°F
V	Mean Flow Velocity	Ft/hr

<u>Greek Symbols</u>

π	Pi	
ρ	Density	lbs/ft^3
μ_f	Dynamic Viscosity At Film Temperature	lbs/ft.hr.
ν	Kinematic Viscosity	ft^2/hr
Θ	Angle	

<u>Dimensionless Numbers</u>

Nu	Nusselt Number ($Nu = \frac{h_c D_H}{K_f}$)
Pr	Prandtl Number ($Pr = \frac{C_p \mu_f}{K_f}$)
Re	Reynolds Number ($Re = \frac{\rho\ VD_H}{\mu_f}$)
f	Fanning Friction Factor ($f = \frac{2g}{4} \frac{D_H}{L} \frac{\Delta p}{V^2}$)
j	Colburn j Factor ($j = \frac{Nu}{RePr^{1/3}}$)
(H/D)	Pitch To Diameter Ratio ($\frac{Ft/360°}{Ft.}$)

REFERENCES

1. Nagaoka, Z. and A. Watanabe: "Maximum Rate of Heat Transfer with Minimum Loss of Energy", Proc. Int. Congr. Refr., 7th Congr., 1936, 3, 1937, pp. 221-295.

2. Margolis, D.: "The Effect of Turbulence Promotors on the Rate of Heat Transfer and the Pressure drop in Straight Tubes", M.Eng. Thesis, Lehigh University, June 1957.

3. Schneider, P. J.: "Conduction Heat Transfer", Addison-Wesley Publishing Company, Inc., First Edition, 1955, pp. 70-72.

4. Kreith, F. and Margolis, D.: "Heat Transfer and Friction in Turbulent Vortex Flow", Applied Scientific Research, Sect. 4, Vol. 8, No. 6, 1959, pp. 457-473.

5. Bhatia, R. M. and P. Kumar: "The Effect of Turbulence Promotors on the Heat Transfer Rates and Pressure Drop in Straight Tubes", B. Tech. Project Report, Indian Inst. of Technology, New Delhi, India, April 1967.

6. Bhatia, R.M., P. Kumar and Y.C. Sud: "Contribution to Swirl Flow Heat Transfer and Friction Factor Calculations" Journal of the Institution of Engineers (India), Vol. 48, No. 1, Part ME1, Sept. 1967, pp. 34-43.

7. Judd, R. L.: "Turbulent Forced Convection Heat Transfer in Annular Passages", M.Eng. thesis, Mechanical Engineering Department, McMaster University, May, 1963.

8. Beckman, W.A., H. Merte, Jr., J. A. Clark: "A Photographic Study of Boiling in an Accelerating System", Technical Report, University of Michigan, pp. 45-46.

9. McAdams: "Heat Transmission", Third Edition, McGraw-Hill Book Company, 1954, page 219, equation (9-10b)* taken from the reference by Colburn A.P., Trans. Am. Inst. Chem. Engrs. 29, 1933, pp. 174-210.

10. von Kármán, T.: "Turbulence and Skin Friction", Journal of Aeronautical Sciences, Vol. 1, No. 1, January, 1934, page 1.

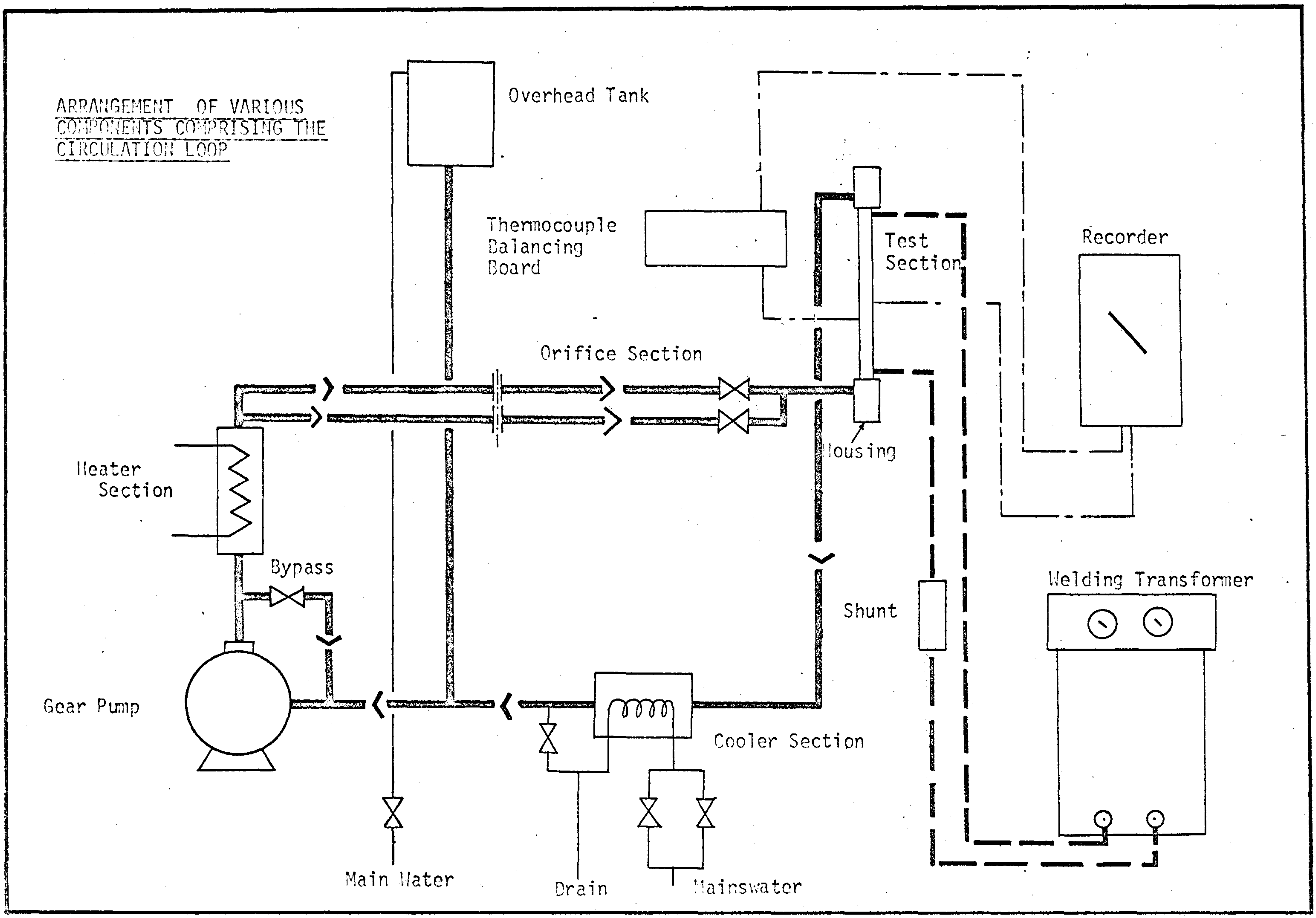
ARRANGEMENT OF VARIOUS COMPONENTS COMPRISING THE CIRCULATION LOOP
Overhead Tank
Thermocouple Balancing Board
Test Section
Recorder
Orifice Section
Housing
Heater Section
Bypass
Shunt
Welding Transformer
Gear Pump
Cooler Section
Main Water
Drain
Mainswater

FIGURE 1.

TEST FACILITY

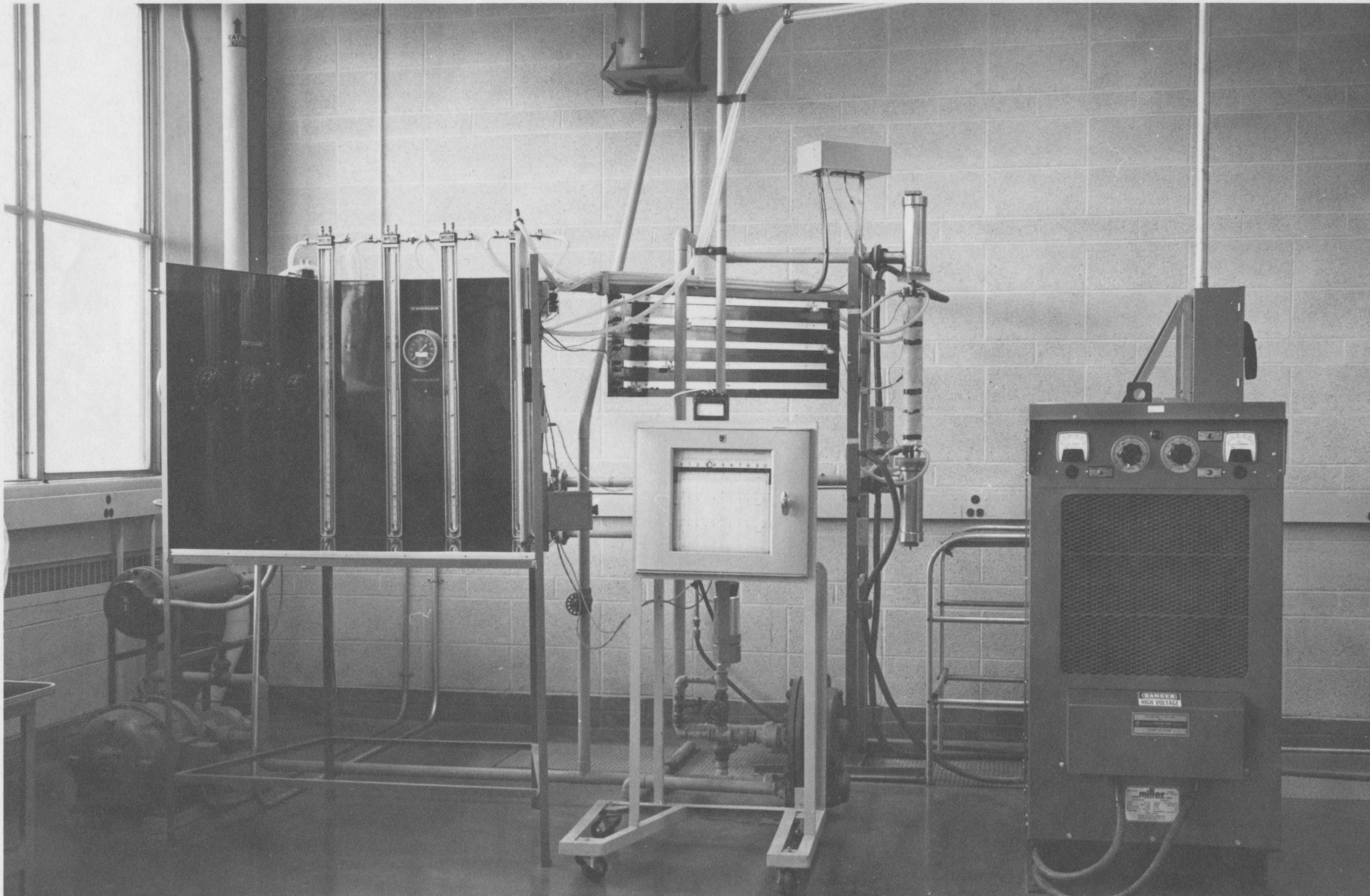

FIGURE 2

TEST SECTION ASSEMBLY

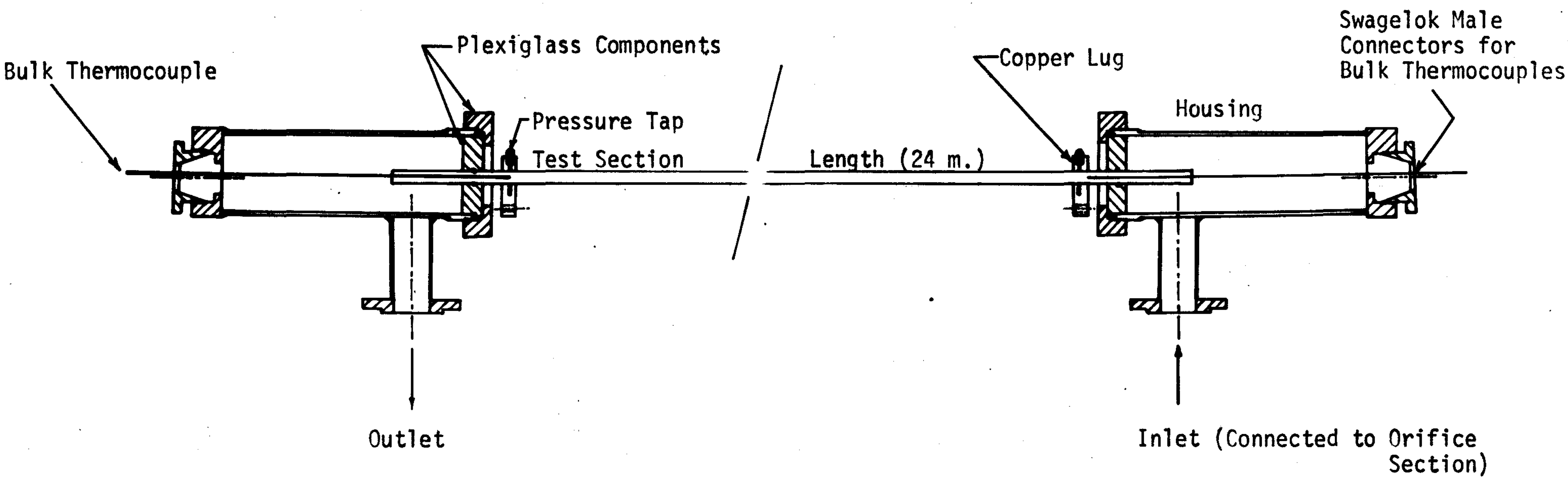

FIGURE 3

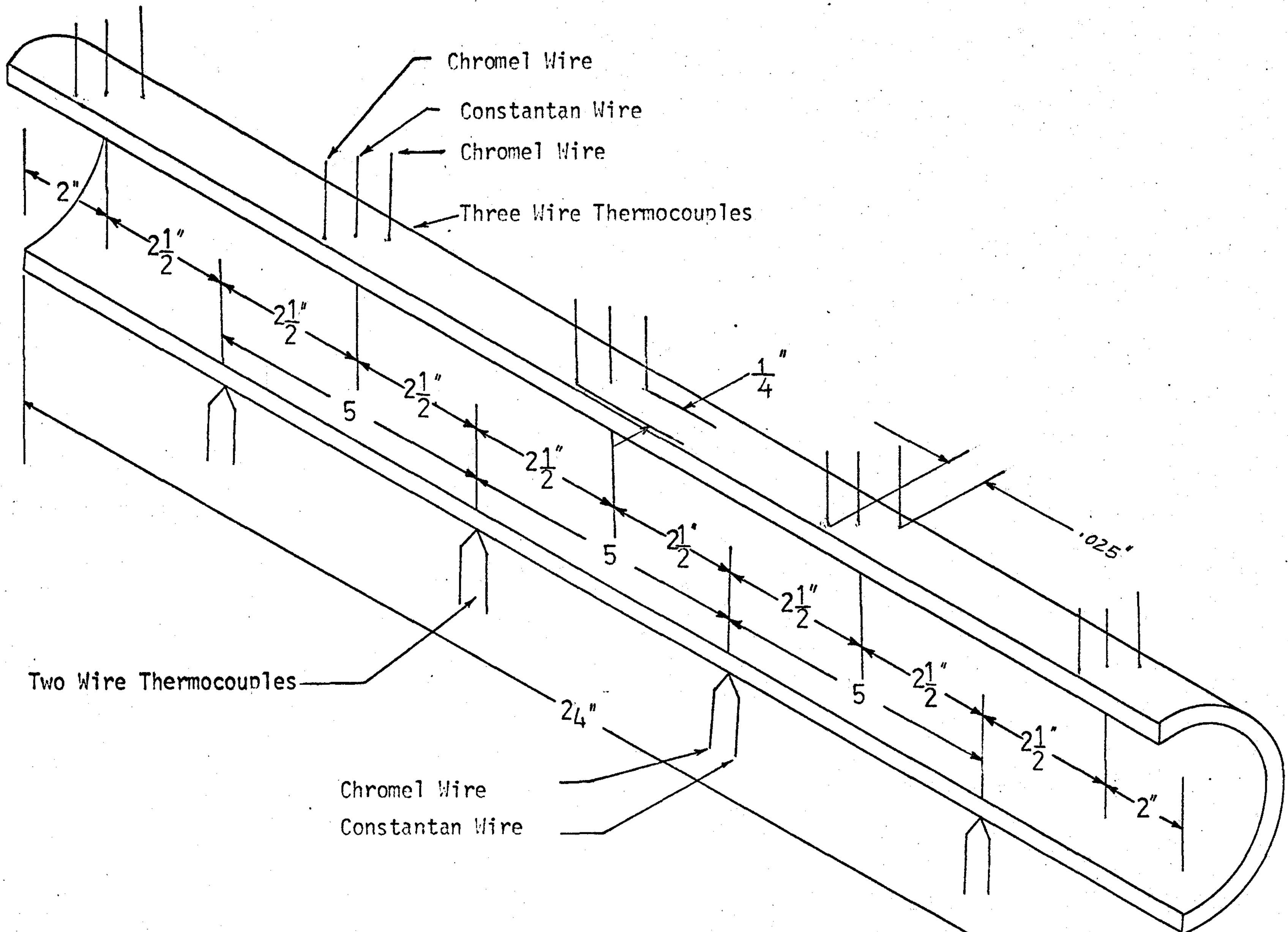

FIGURE 4

LOCATION OF NINE TUBE WALL THERMOCOUPLES

DEVELOPMENT OF TUBE SURFACE

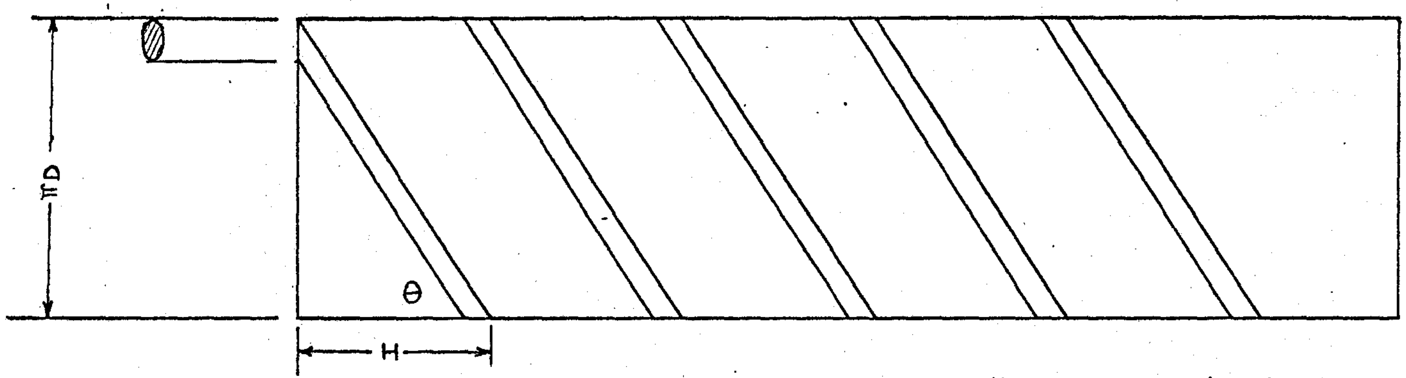

$$\cos \Theta = \frac{H}{\sqrt{(\pi D)^2 + H^2}} = \frac{(H/D)}{\sqrt{\pi^2 + (H/D)^2}}$$

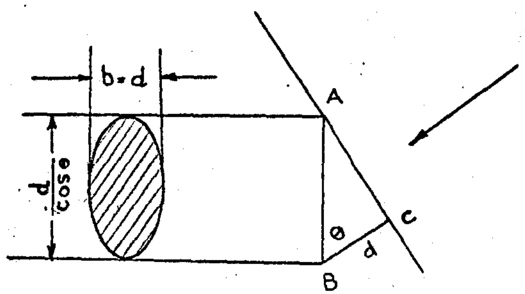

Enlargement of Wire Cross Section

$$AB = \frac{d}{\cos \Theta}$$

FIGURE 5

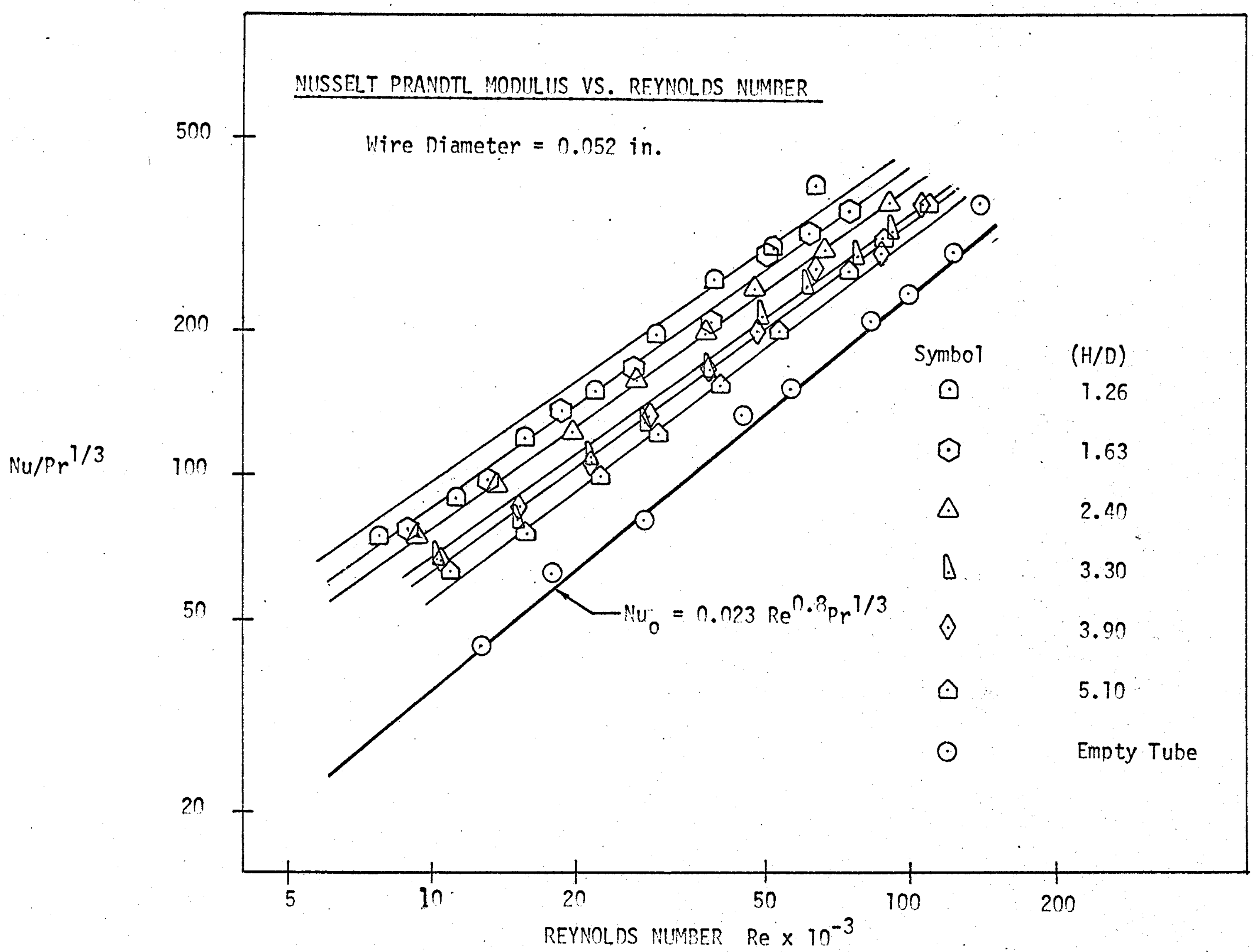
NUSSELT PRANDTL MODULUS VS. REYNOLDS NUMBER
Wire Diameter = 0.052 in.
$Nu/Pr^{1/3}$
500
200
100
50
20
5
10
20
50
100
200
REYNOLDS NUMBER $Re \times 10^{-3}$
$Nu_o = 0.023\ Re^{0.8} Pr^{1/3}$
Symbol
(H/D)
1.26
1.63
2.40
3.30
3.90
5.10
Empty Tube

FIGURE 6

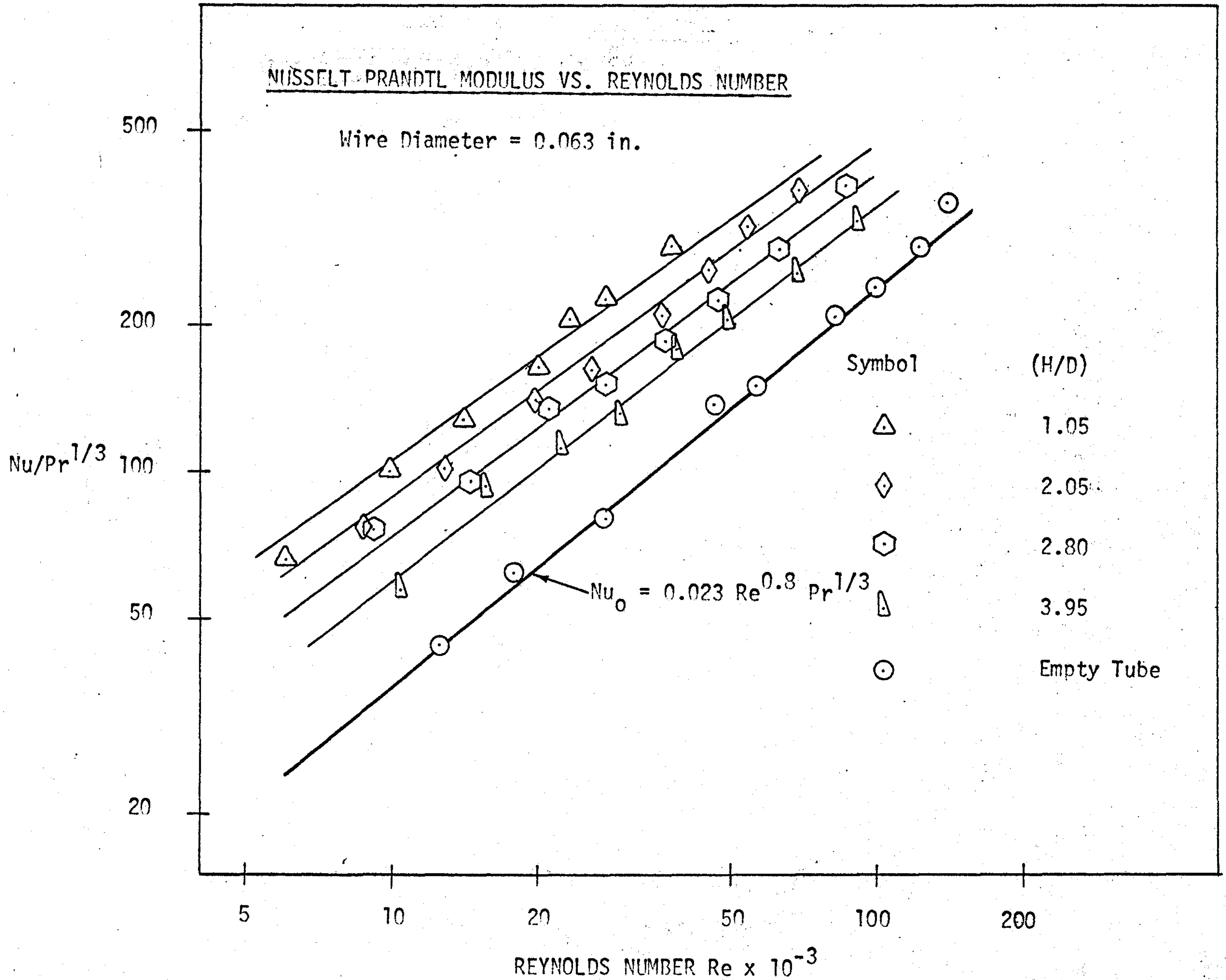
NUSSELT-PRANDTL MODULUS VS. REYNOLDS NUMBER
Wire Diameter = 0.063 in.
$Nu/Pr^{1/3}$
500
200
100
50
20
5
10
20
50
100
200
REYNOLDS NUMBER Re x 10^{-3}
$Nu_o = 0.023\ Re^{0.8}\ Pr^{1/3}$
Symbol
(H/D)
1.05
2.05
2.80
3.95
Empty Tube

FIGURE 7

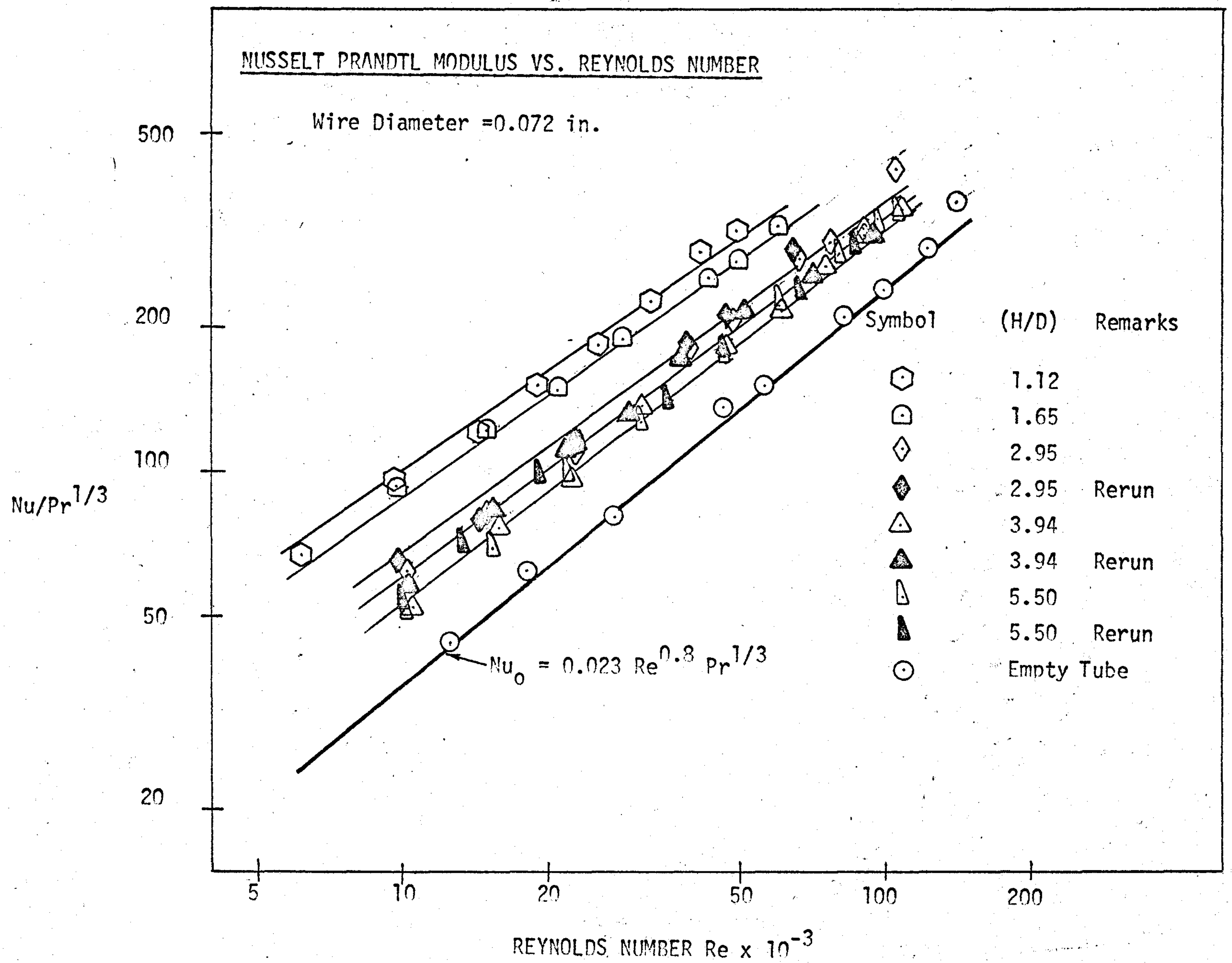
NUSSELT PRANDTL MODULUS VS. REYNOLDS NUMBER
Wire Diameter =0.072 in.
500
200
100
50
20
Nu/Pr$^{1/3}$
5
10
20
50
100
200
REYNOLDS NUMBER Re x 10^{-3}
$Nu_o = 0.023 Re^{0.8} Pr^{1/3}$
Symbol
(H/D)
Remarks
1.12
1.65
2.95
2.95 Rerun
3.94
3.94 Rerun
5.50
5.50 Rerun
Empty Tube

FIGURE 8

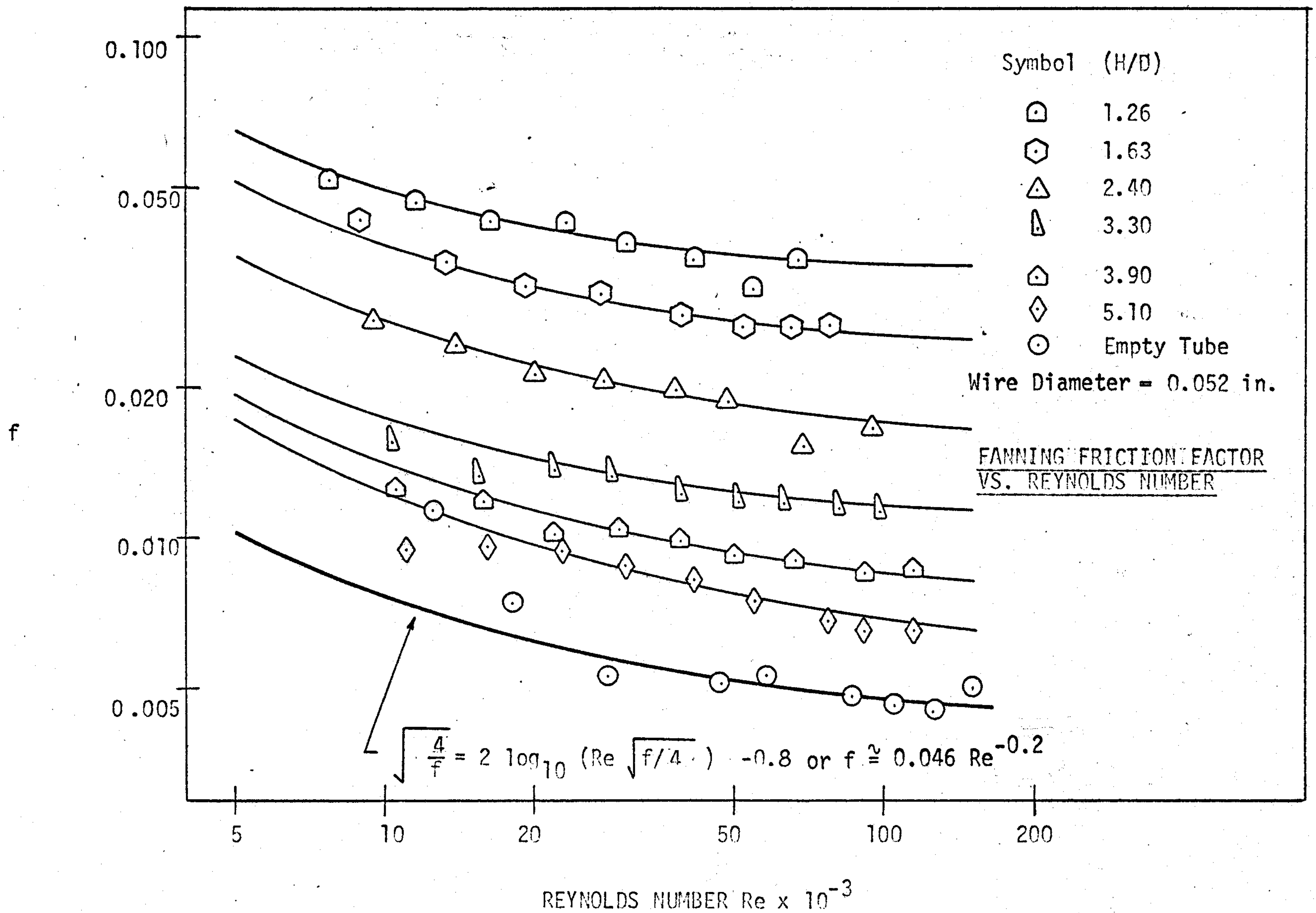
0.100
0.050
0.020
0.010
0.005
f
Symbol (H/D)
1.26
1.63
2.40
3.30
3.90
5.10
Empty Tube
Wire Diameter = 0.052 in.
FANNING FRICTION FACTOR
VS. REYNOLDS NUMBER
$\sqrt{\frac{4}{f}} = 2 \log_{10} (Re \sqrt{f/4}) - 0.8$ or $f \cong 0.046\ Re^{-0.2}$
5
10
20
50
100
200
REYNOLDS NUMBER $Re \times 10^{-3}$

FIGURE 9

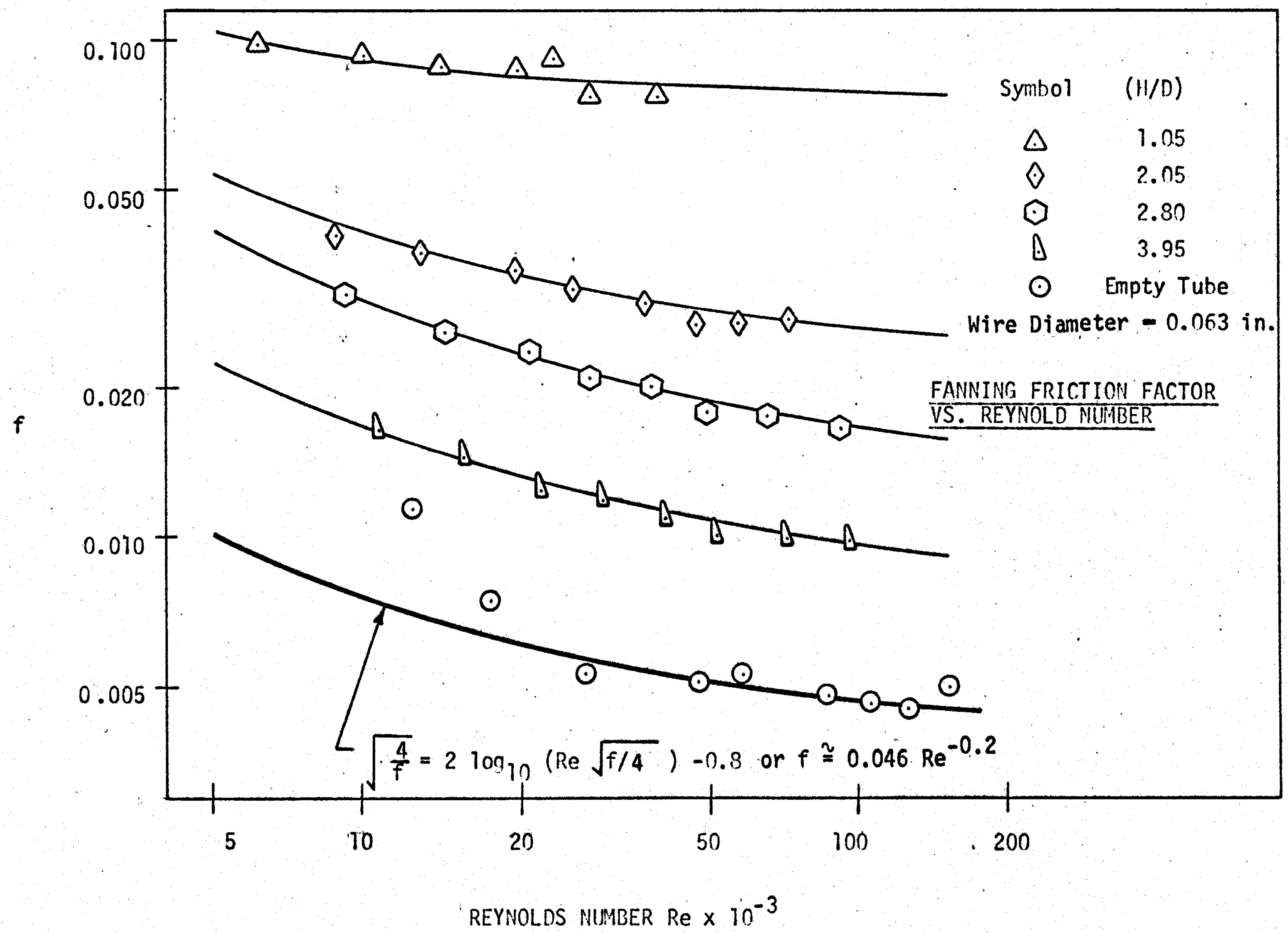
0.100
0.050
0.020
0.010
0.005
f
Symbol (H/D)
1.05
2.05
2.80
3.95
Empty Tube
Wire Diameter = 0.063 in.
FANNING FRICTION FACTOR
VS. REYNOLD NUMBER
$\sqrt{\frac{4}{f}} = 2 \log_{10} (Re \sqrt{f/4}) - 0.8$ or $f \cong 0.046 Re^{-0.2}$
5
10
20
50
100
200
REYNOLDS NUMBER $Re \times 10^{-3}$

FIGURE 10

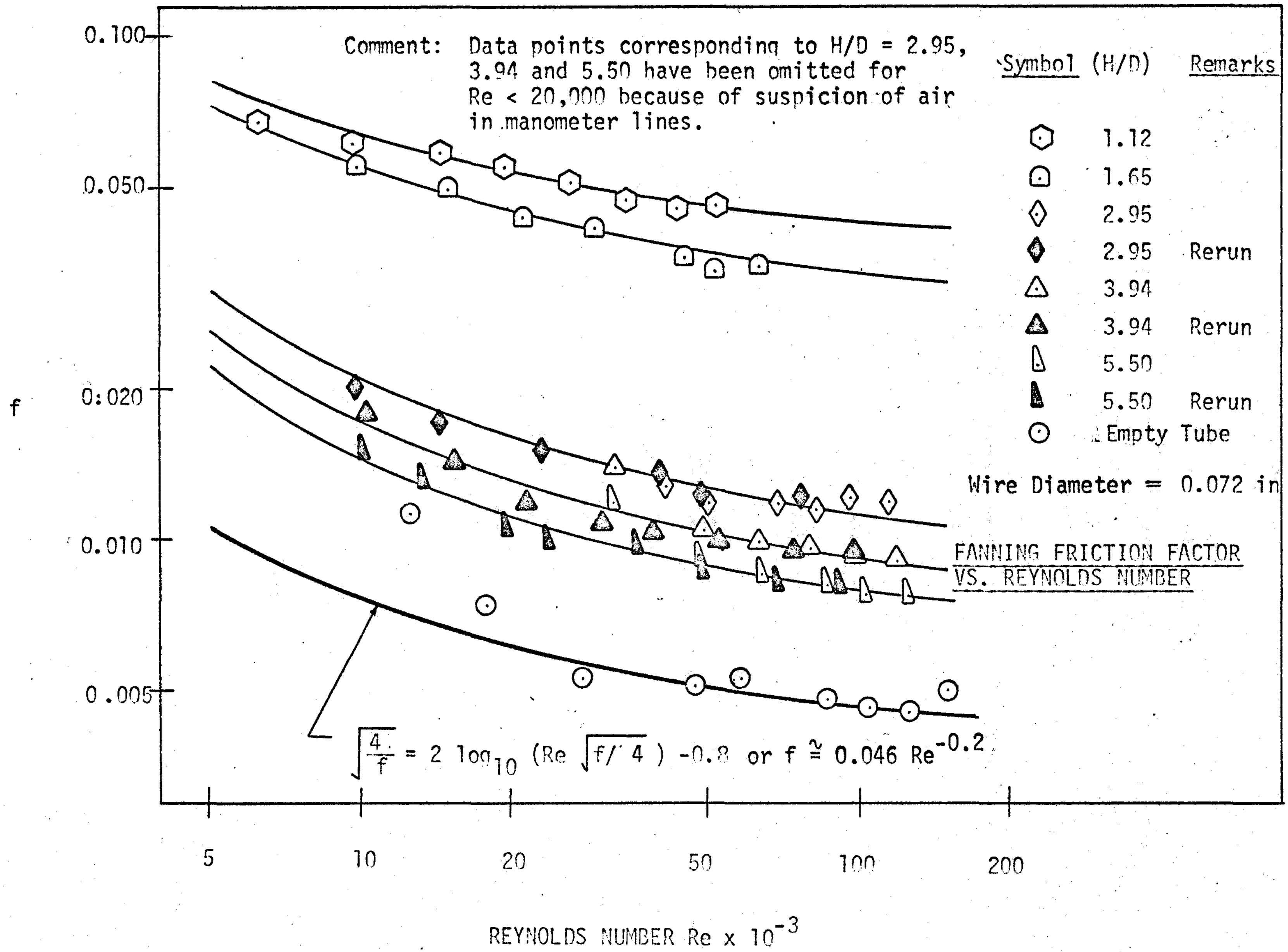
Comment: Data points corresponding to H/D = 2.95, 3.94 and 5.50 have been omitted for Re < 20,000 because of suspicion of air in manometer lines.
Symbol
(H/D)
Remarks
1.12
1.65
2.95
2.95 Rerun
3.94
3.94 Rerun
5.50
5.50 Rerun
Empty Tube
Wire Diameter = 0.072 in
FANNING FRICTION FACTOR VS. REYNOLDS NUMBER
f
0.100
0.050
0.020
0.010
0.005
5
10
20
50
100
200
REYNOLDS NUMBER Re x 10^{-3}
$\sqrt{\frac{4}{f}} = 2 \log_{10} (Re \sqrt{f/4}) - 0.8$ or $f \cong 0.046\ Re^{-0.2}$

FIGURE 11.

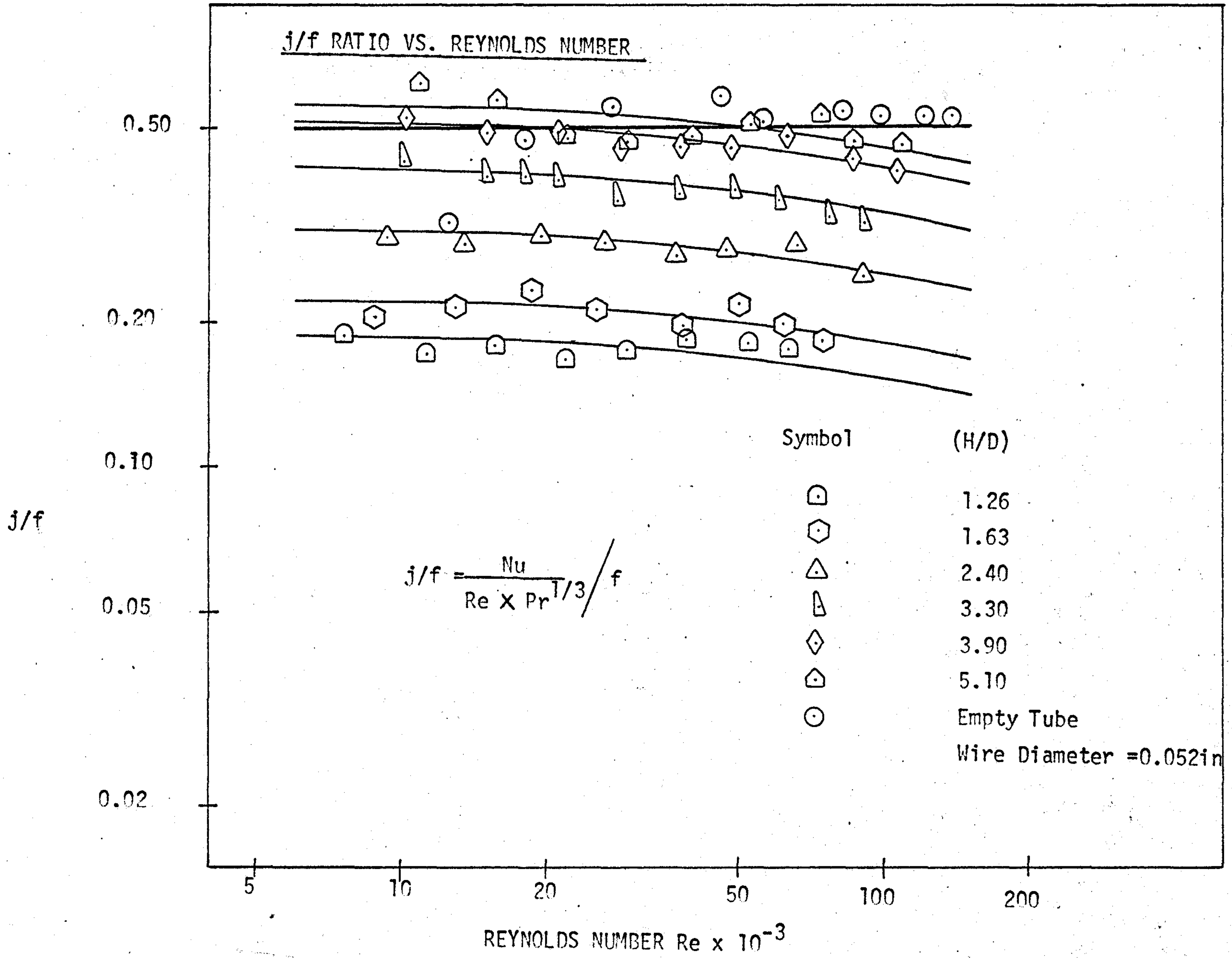

j/f RATIO VS. REYNOLDS NUMBER
0.50
0.20
0.10
0.05
0.02
j/f
j/f = Nu / Re X Pr1/3 / f
Symbol
(H/D)
1.26
1.63
2.40
3.30
3.90
5.10
Empty Tube
Wire Diameter =0.052in
5
10
20
50
100
200
REYNOLDS NUMBER Re x 10-3

FIGURE 12

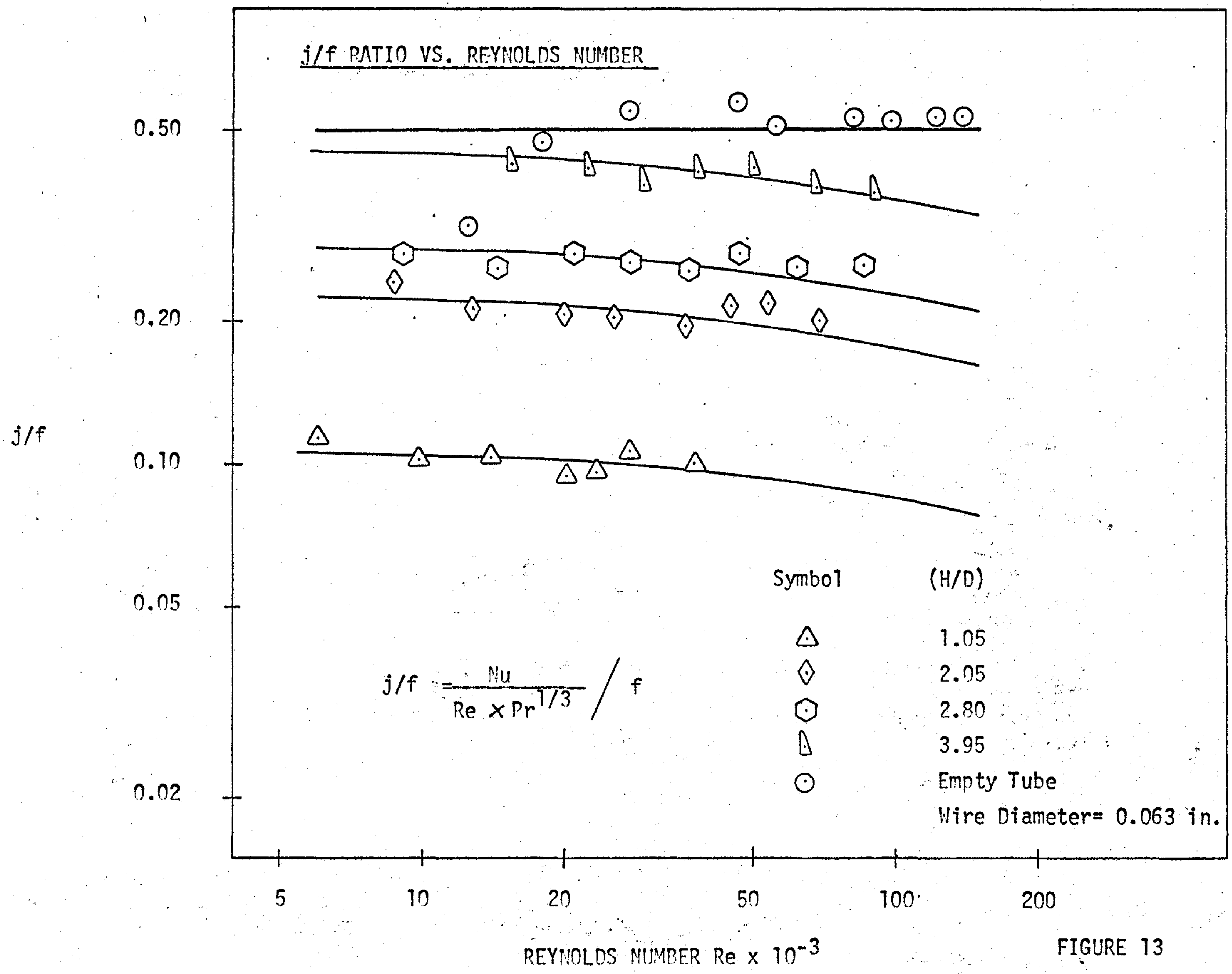

j/f RATIO VS. REYNOLDS NUMBER
0.50
0.20
0.10
0.05
0.02
j/f
Symbol
(H/D)
1.05
2.05
2.80
3.95
Empty Tube
Wire Diameter= 0.063 in.
$j/f = \frac{Nu}{Re \times Pr^{1/3}} / f$
5
10
20
50
100
200
REYNOLDS NUMBER Re x 10^{-3}

FIGURE 13

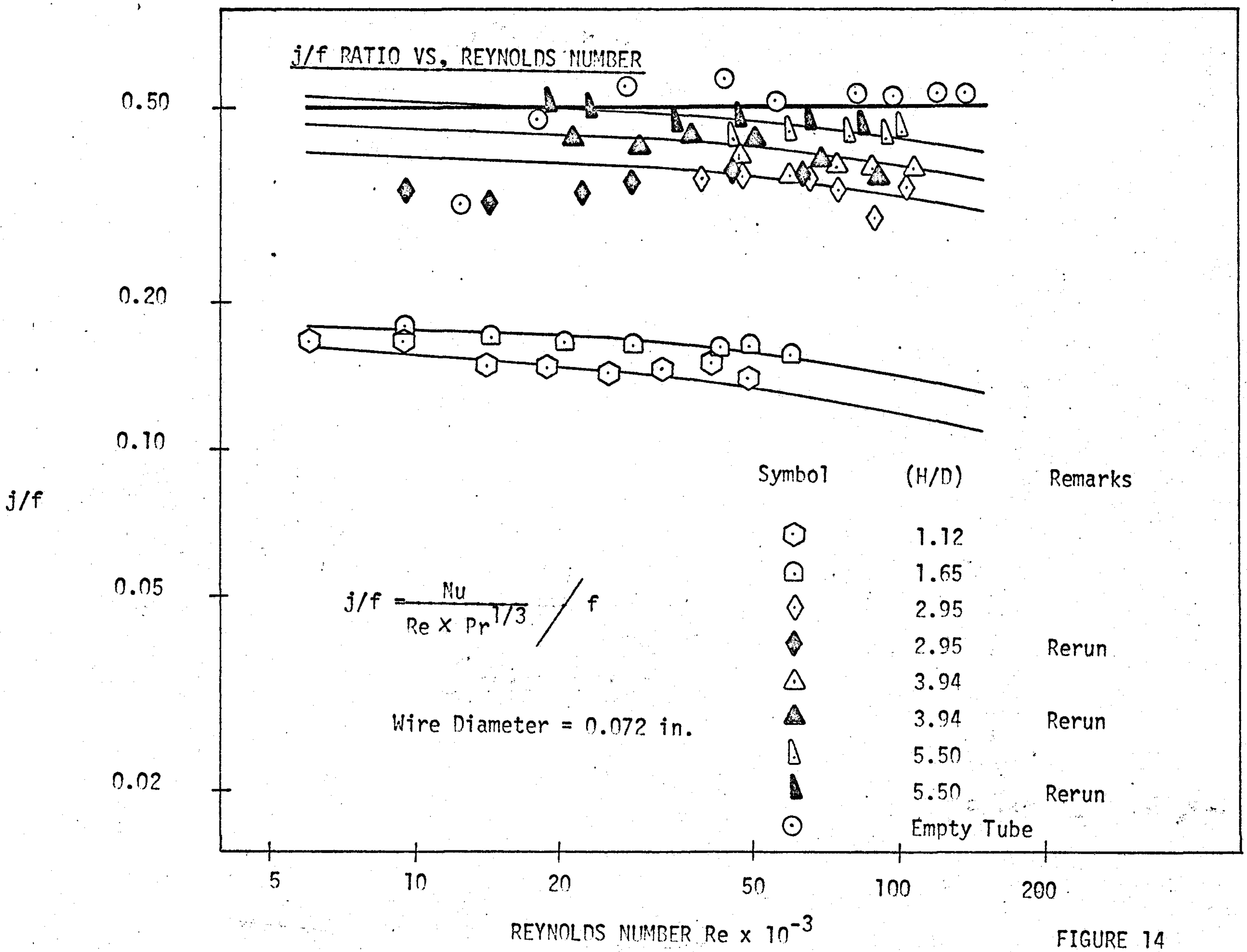

j/f RATIO VS. REYNOLDS NUMBER
0.50
0.20
0.10
0.05
0.02
j/f
$j/f = \frac{Nu}{Re \times Pr^{1/3}} \Big/ f$
Wire Diameter = 0.072 in.
Symbol
(H/D)
Remarks
1.12
1.65
2.95
2.95 Rerun
3.94
3.94 Rerun
5.50
5.50 Rerun
Empty Tube
5
10
20
50
100
200
REYNOLDS NUMBER Re x 10^{-3}

FIGURE 14

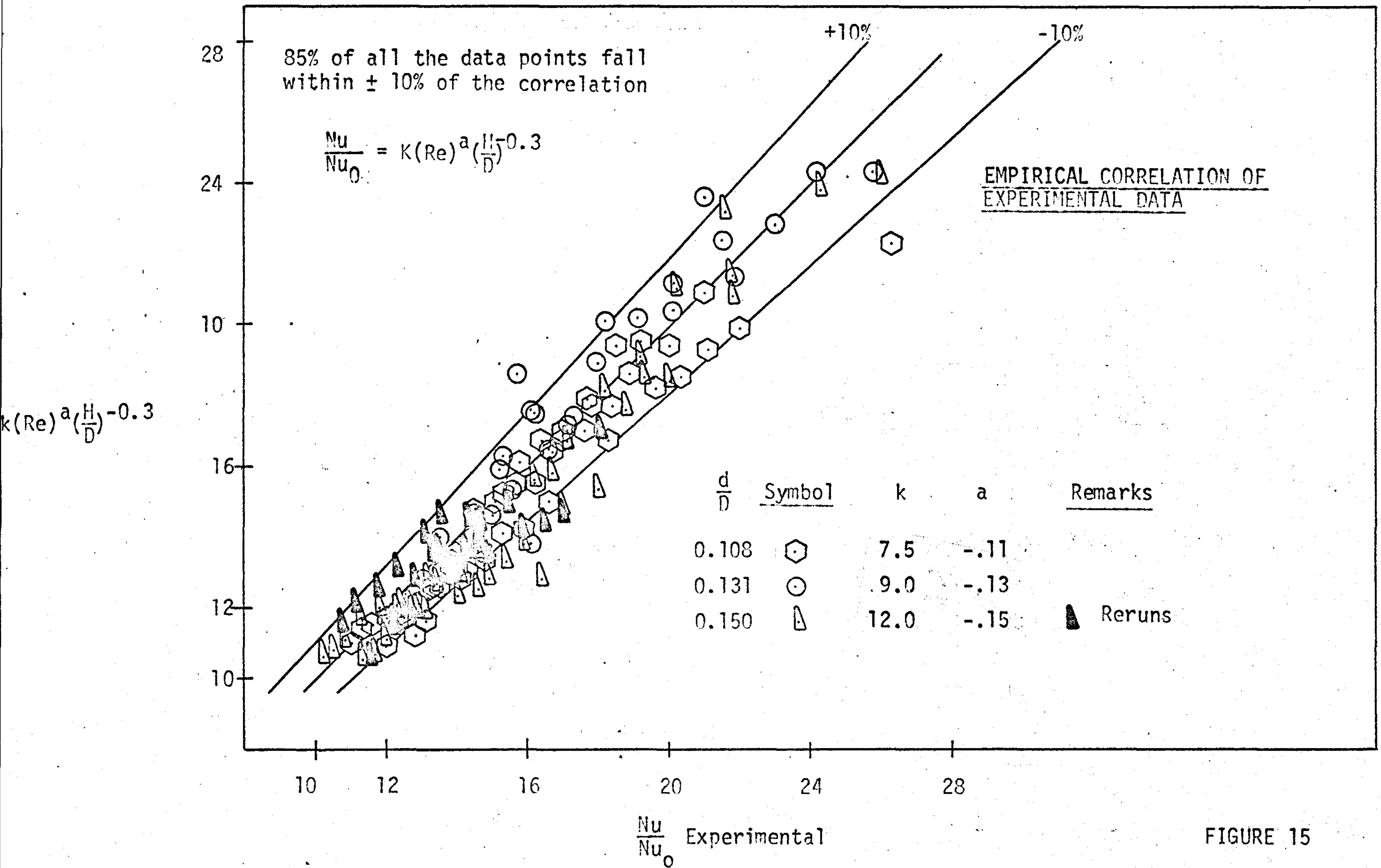
85% of all the data points fall
within ± 10% of the correlation
$\frac{Nu}{Nu_0} = K(Re)^a(\frac{H}{D})^{-0.3}$
+10%
-10%
EMPIRICAL CORRELATION OF
EXPERIMENTAL DATA
$k(Re)^a(\frac{H}{D})^{-0.3}$
28
24
10
16
12
10
10
12
16
20
24
28
$\frac{d}{D}$ Symbol k a Remarks
0.108 7.5 -.11
0.131 9.0 -.13
0.150 12.0 -.15 Reruns
$\frac{Nu}{Nu_o}$ Experimental

FIGURE 15

APPENDIX A

Calibration of Orifice Plates

The orifice plates were calibrated by passing water through the orifices and collecting it in a tank. The mass flow collected in the tank was determined by weighing and the corresponding pressure differential was measured by a mercury differential manometer.

Calibration points were obtained up to 10 in. of mercury pressure differential for the orifice plate in 1-1/2 in. pipe. The straight line correlation was extrapolated up to 36 in. of mercury pressure drop, since it was not possible to obtain calibration points for the range 10 in. mercury pressure differential to 36 in. of mercury pressure differential. Figure 16 shows the calibration curves for the two orifice plates.

CALIBRATION CURVES FOR THE ORIFICE PLATES

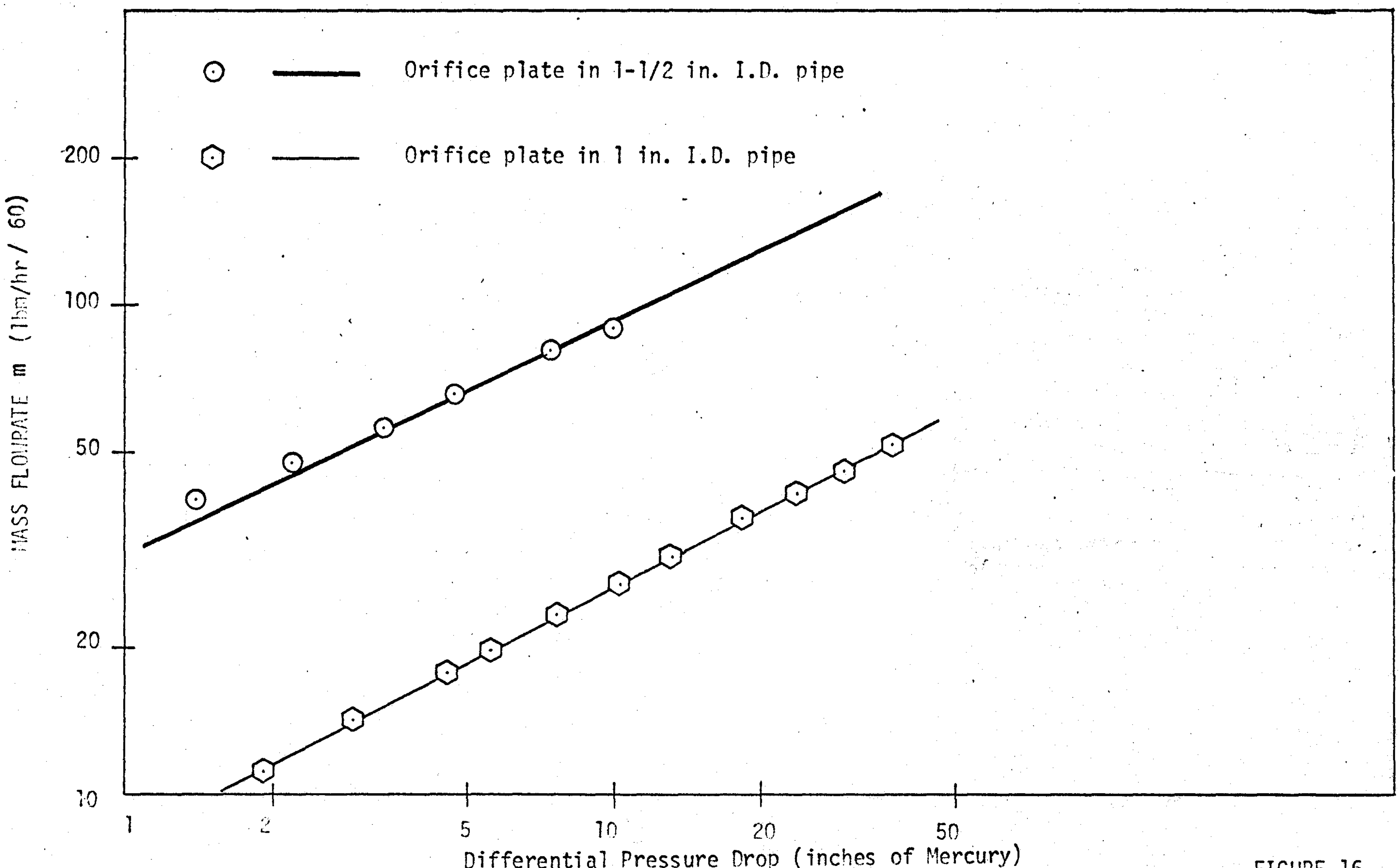

FIGURE 16

APPENDIX B

Effect Of Various Mass Flow Rates On The Position Of The Coil

A simple experiment was performed to ascertain whether the turbulence promotor was affected by the flow in the tube or stayed in position. A coil was inserted in a plexiglass tube 5/8" O.D. and 1/2" I.D. and water was allowed to pass through it at different mass flow rates. Figure 17 on the following page shows that the coil had enough tension to hold itself against the tube wall under mass flow conditions ranging from a minimum of zero to a maximum of 6600 lbs/hour.

POSITION OF COIL AT VARIOUS MASS FLOW RATES

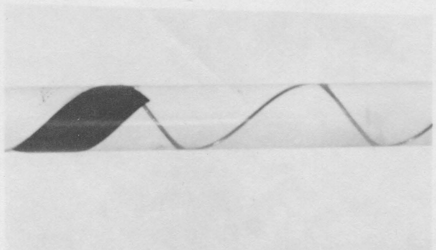

ZERO MASS FLOW RATE

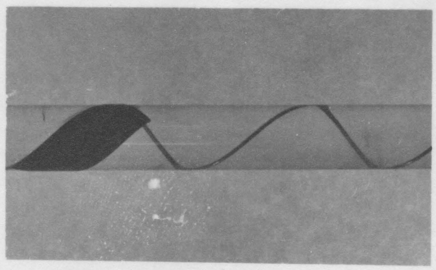

MASS FLOW RATE = 2200 lbs/hr.

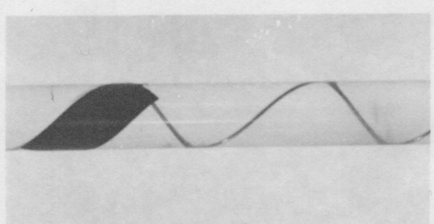

MASS FLOW RATE = 4200 lbs/hr.

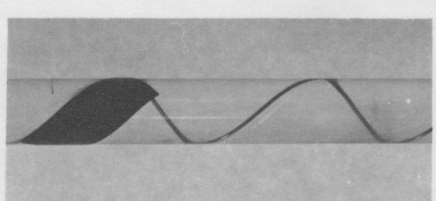

MASS FLOW RATE = 6600 lbs/hr.

FIGURE 17

APPENDIX C

Analysis of Temperature Data

The nine tube wall thermocouples spotwelded on the outside of the test section were positioned along the length of the tube in two diametrically opposite groups as shown in Figure 4. Figure 18 compares the temperatures measured with these two groups of thermocouples for one representative test condition.

The bulk temperatures at the inlet and the outlet sections were measured in two different manners as explained in Section 3.3 of Chapter 3. The first method employed the use of two bulk thermocouples and the second method made use of two precision mercury-in-glass thermometers inserted in thermometer wells upstream and downstream of the test section. Figure 19 compares the temperatures measured by bulk thermocouples and bulk thermometers in a typical test. Bulk temperature rise was assumed to be linear as the heat flux was uniform.

Figure 20 shows a plot used to evaluate the film temperature drop ΔT_f and the film temperature T_f. It was observed that the rate of wall temperature rise was identical to the rate of bulk temperature rise about 12 in. from the inlet section and further on. This observation indicated that fully developed thermal conditions existed in this region.

TABLE III

DATA PERTINENT TO TEMPERATURE DATA ANALYSIS

	m lbs/hr.	Δp_1 "Hg	Δp_2 "Hg	Δp_3 "Hg	E Volts	I Amps	TEMPERATURE DATA										
							BULK TEMPS.		SURFACE TEMPERATURES								
							T_i °F	T_o °F	T_1 °F	T_2 °F	T_3 °F	T_4 °F	T_5 °F	T_6 °F	T_7 °F	T_8 °F	T_9 °F
THERMOMETERS	2383	6.7	6.8	7.3	16.0	362.0	85.0	93.6									
THERMOCOUPLES							84.5	93.1	107.0	110.5	110.0	112.0	111.6	114.0	113.2	114.2	115.4

COMPARISON OF THE TWO WIRE AND THREE WIRE THERMOCOUPLES

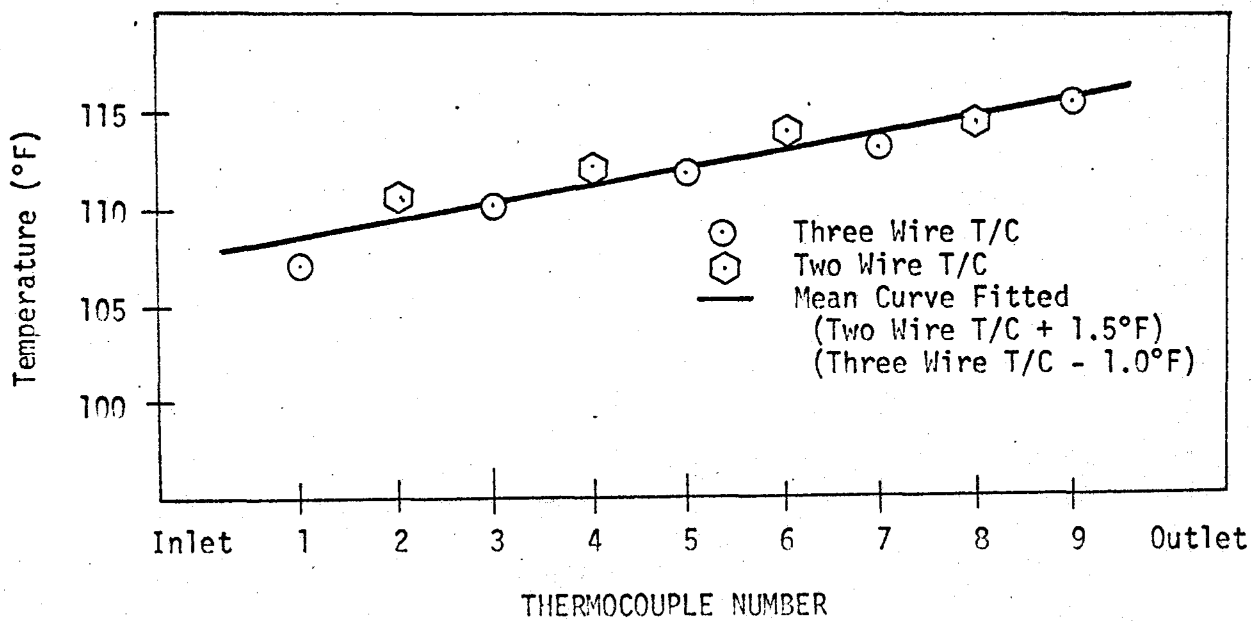

FIGURE 18

COMPARISON OF BULK TEMPERATURES MEASURED

WITH BULK THERMOMETERS AND BULK THERMOCOUPLES

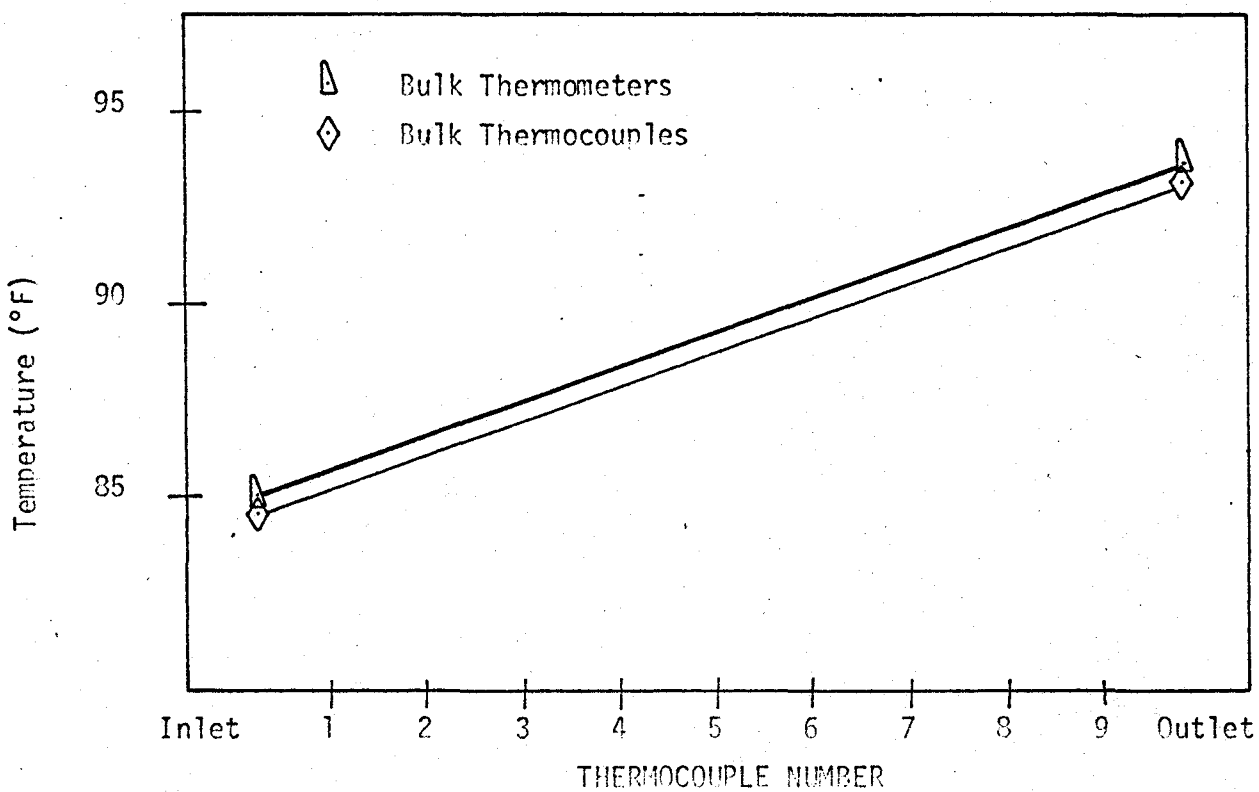

FIGURE 19

EVALUATION OF ΔT_f AND T_f

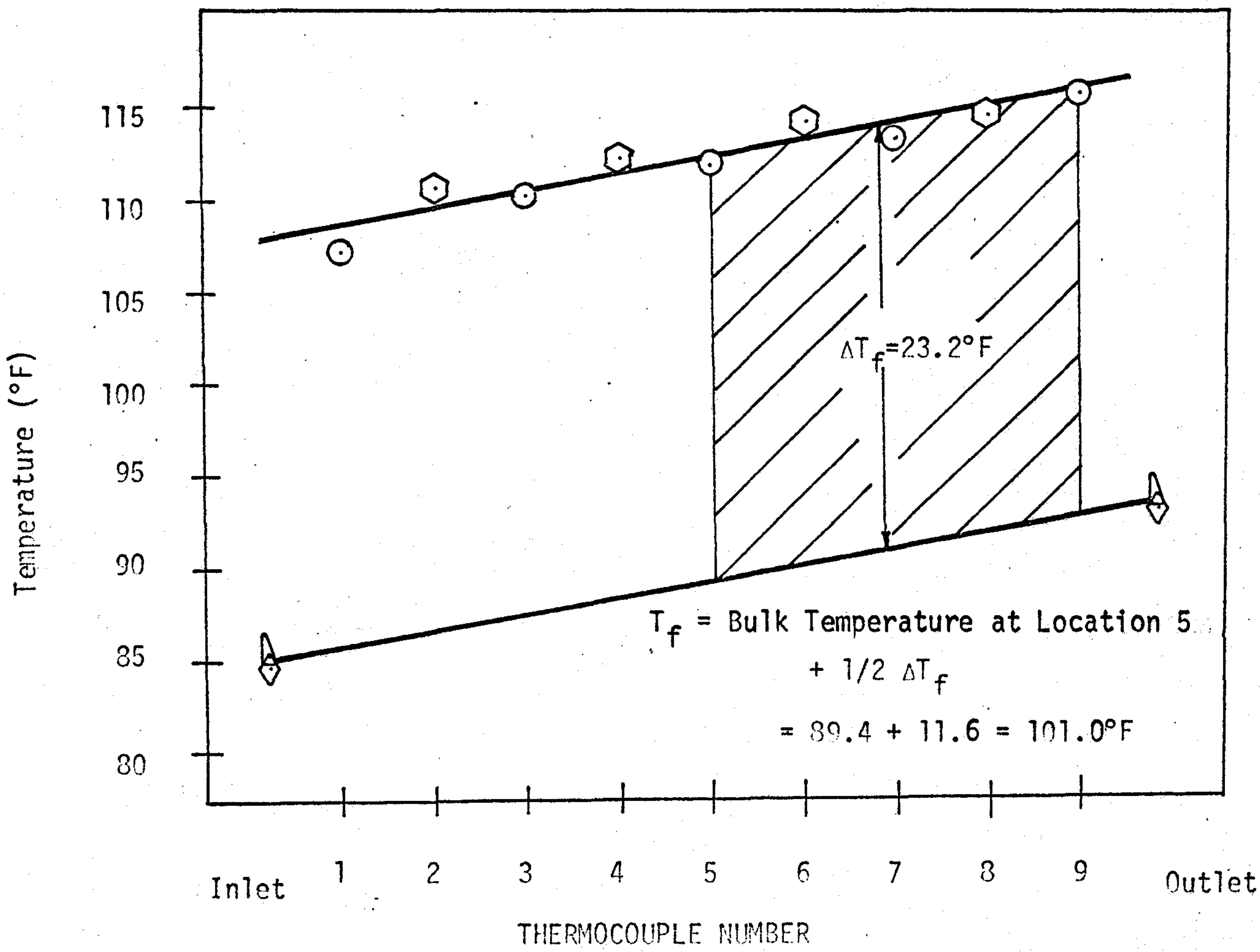

FIGURE 20

APPENDIX D

Sample Calculations

The calculations in this appendix are based upon the following set of data:

Mass flow rate - m = 39.8 lbs/min. = 2388 lbs/hour

Pressure drop Δp_1 = 6.7 in. Hg.

Pressure drop Δp_2 = 6.8 in. Hg.

Pressure drop Δp_3 = 7.3 in. Hg.

Potential drop - E = 16.0 volts

Current flow - I = 362 amps.

Inlet temperature - T_i = 85.0°F

Outlet temperature- T_o = 93.6°F

H/D Ratio H/D = 1.63

Wire diameter d = 0.052 in.

Wall temperature distribution in Figure 18 of Appendix C

ΔT_B = 93.6 - 85.0 = 8.6°F

ΔT_f = 23.2°F Figure 20 of Appendix C

T_f = 101.0°F Figure 20 of Appendix C

Corrected ΔT_f = 23.2 - 3.6 = 19.6°

Corrected T_f = 101.0 - 3.6 = 97.4°

(a) Area of Flow

$$\text{Cos}\Theta = \frac{1.63}{\sqrt{(1.63)^2 + \pi^2}} = 0.345$$

The major diameter $a = \frac{d}{\text{Cos } \Theta} = \frac{0.05}{0.34} = 0.151$ in.

The minor diameter b = d = 0.0520 in.

Area of flow $A = \frac{\pi}{4}(D^2 - ab) = \frac{\pi}{4}[0.48^2 - 0.1509 \times 0.052]\ in^2$

$$= 0.00126\ ft^2$$

(b) Hydraulic Diameter

$$D_H = 4 \times \frac{\text{Cross Sectional Flow Area}}{\text{Wetted Perimeter}}$$

$$\text{Wetted Perimeter } P = \pi D + \pi \sqrt{\frac{a^2 + b^2}{2}}$$

$$= 1.508 + .3729 = 1.881 \text{ in.} = 0.157 \text{ ft.} \qquad (6.4)$$

$$D_H = 0.386 \text{ in.} = 0.032 \text{ ft.} \qquad (6.5)$$

(c) Reynolds Number

$$Re = \frac{\dot{m}D_H}{A\mu_f} = \frac{2388 \times 0.032 \times 10^3}{0.00126 \times .472 \times 3600} = 35{,}700 \qquad (6.6)$$

(d) Film Heat Transfer Coefficient

$$\left(\frac{Q}{A_S}\right) = \frac{3.413 \times 16 \times 362 \times 144}{\pi \times 24 \times 0.48} = 79{,}295 \text{ BTU/hr. ft}^2 \qquad (6.8)$$

$$h_c = \frac{79295}{20.0} = 3965 \text{ BTU/hr. ft}^2\,{}^\circ F \qquad (6.7)$$

$$\left(\frac{Q}{A_S}\right) = \frac{2388 \times 0.998 \times 8.6}{\pi \times 24 \times 0.48} = 81{,}550 \text{ BTU/hr.ft}^2 \qquad (6.9)$$

(e) Nusselt Prandtl Modulus

$$\frac{Nu}{Pr^{1/3}} = \frac{\frac{h_c\ D_H}{K_f}}{Pr^{1/3}} = \frac{\frac{3965 \times 0.032}{.364}}{(4.65)^{1/3}}$$

$$= \frac{3965 \times 0.032}{1.67 \times .364} = 209 \qquad (6.10)$$

(f) Colburn j Factor

$$j = \frac{Nu}{Pr^{1/3}} / Re = \frac{209}{35700} = .00585 \qquad (6.11)$$

(g) Fanning Friction Factor

$$f = \frac{\Delta p}{4} \frac{D_H}{L} \frac{2g}{V^2}$$

$$\Delta p = \frac{\Delta p_1 + \Delta p_2 + \Delta p_3}{3} = \frac{6.7 + 6.8 \div 7.3}{3} = 6.9 \text{ in. of Hg.}$$

$$= \frac{6.9 \times 13.6}{12} = 7.86 \text{ ft. of water}$$

$$V = \frac{m}{\rho A} = \frac{2388}{62.4 \times .00126}$$

$$= 30{,}372 \text{ ft/hr.}$$

$$f = \frac{7.86}{2} \times \frac{0.03216}{2} \times \frac{32.2 \times 3.6^2}{30{,}372^2} = .0286 \qquad (6.12)$$

(h) j/f Ratio

$$j/f = \frac{.00585}{.0286} = 0.218$$

APPENDIX E

DERIVED RESULTS

Wire Size	H/D Ratio	Test	Re x 10^{-3}	Pr	$Nu/Pr^{1/3}$	j	f	j/f
		1	7.6	4.81	73.5	.00960	0.0515	.186
		2	11.2	4.66	89.0	.00793	0.0466	.170
		3	15.6	4.64	118.0	.00756	0.0427	.177
		4	21.9	4.50	149.0	.00680	0.0412	.165
0.052 in.	1.26	5	29.2	4.48	194.0	.00664	0.0384	.173
		6	38.7	4.52	253.0	.00652	0.0359	.182
		7	51.5	4.59	293.0	.00569	0.0313	.181
		8	63.0	4.66	395.0	.00630	0.0359	.175
		1	8.8	4.66	77	.0087	0.0430	.202
		2	12.9	4.50	97	.0075	0.0355	.212
		3	18.6	4.39	136	.0073	0.0319	.229
		4	26.2	4.32	167	.0064	0.0306	.208
0.052 in.	1.63	5	38.0	4.33	207	.00545	0.0278	.196
		6	49.5	4.31	284	.00575	0.0264	.217
		7	61.3	4.29	315	.00514	0.0263	.195
		8	73.8	4.41	350	.00475	0.0265	.179
		1	92.7	5.00	74	.0080	0.0271	.294
		2	13.6	4.88	94	.0069	0.0241	.286
		3	19.6	4.73	122	.0062	0.0211	.295
		4	26.5	4.73	158	.0060	0.0206	.288
0.052 in.	2.40	5	37.0	4.78	198	.0054	0.0199	.269
		6	46.7	4.88	241	.0052	0.0186	.278
		7	66.1	4.73	290	.0044	0.0152	.288
		8	89.5	4.81	362	.0040	0.0166	.244

. . . Cont'd ...

APPENDIX E

DERIVED RESULTS

Wire Size	H/D Ratio	Test	Re x 10^{-3}	Pr	$Nu/Pr^{1/3}$	j	f	j/f
		1	101.0	5.00	66	.0065	0.0154	.425
		2	15.0	4.81	80	.0052	0.0133	.393
		3	21.2	4.73	107	.0051	0.0137	.385
		4	27.7	4.68	128	.0046	0.0133	.347
0.052 in	3.30	5	37.6	4.73	165	.0044	0.0122	.360
		6	49.0	4.88	212	.0043	0.0118	.367
		7	60.5	4.83	248	.0041	0.0117	.350
		8	77.2	4.83	283	.0037	0.0114	.322
		9	91.2	4.68	324	.0035	0.0113	.314
		1	10.3	5.08	66	.0065	0.0124	.520
		2	15.1	4.83	86	.0057	0.0118	.485
		3	21.3	4.73	106	.0050	0.0102	.487
		4	28.5	4.63	132	.0047	0.0104	.447
0.052 in.	3.90	5	37.7	4.73	166	.0044	0.0098	.450
		6	48.2	4.88	198	.0041	0.0092	.445
		7	62.8	4.83	268	.0043	0.0090	.475
		8	85.6	4.83	309	.0036	0.0085	.424
		9	105.5	4.68	361	.0034	0.0086	.400
		1	10.9	5.08	63	.0058	0.00939	.615
		2	15.7	4.83	75	.0048	0.00959	.500
		3	22.1	4.64	98	.0045	0.00939	.473
		4	29.6	4.64	121	.0041	0.00880	.464
0.052 in.	5.10	5	40.0	4.70	155	.0039	0.00821	.475
		6	52.8	4.76	198	.0037	0.00746	.500
		7	73.5	4.83	261	.0036	0.00679	.524
		8	86.7	4.68	304	.0035	0.00752	.462
		9	107.6	4.65	370	.0034	0.00751	.458

... Cont'd ...

APPENDIX E

DERIVED RESULTS

Wire Size	H/D Ratio	Test	Re x 10^{-3}	Pr	$Nu/Pr^{1/3}$	j	f	j/f
		1	6.0	4.78	66	.0110	0.0978	.113
		2	9.85	4.64	100	.0100	0.0922	.102
		3	14.00	4.62	127	.0091	0.0878	.103
		4	20.2	4.62	164	.0081	0.0866	. 94
0.063 in.	1.05	5	23.3	4.64	205	.0088	0.0912	.096
		6	27.6	4.56	225	.0082	0.0762	.107
		7	37.5	4.59	288	.0077	0.0761	.100
		1	8.7	5.02	77	.0089	0.0402	.240
		2	12.8	4.90	101	.0079	0.0374	.212
		3	19.9	4.81	140	.0074	0.0342	.205
		4	25.6	4.78	161	.0063	0.0314	.201
0.063 in.	2.05	5	36.0	4.94	208	.0058	0.0296	.195
		6	45.1	5.02	259	.0057	0.0267	.215
		7	54.0	5.08	317	.0059	0.0269	.218
		8	68.7	5.00	375	.0055	0.0273	.200
		1	9.1	5.00	76	.0084	0.0307	.273
		2	14.4	4.84	95	.0066	0.0256	.257
		3	21.0	4.68	134	.0064	0.0233	.274
0.063 in.	2.80	4	27.6	4.73	150	.0055	0.0208	.262
		5	36.6	4.73	184	.0051	0.0200	.252
		6	46.9	4.71	223	.0050	0.0178	.278
		7	62.5	4.94	285	.0046	0.0176	.258
		8	86.0	4.83	383	.0044	0.0165	.260

... Cont'd ...

APPENDIX E

DERIVED RESULTS

Wire Size	H/D Ratio	Test	Re x 10^{-3}	Pr	Nu/$Pr^{1/3}$	j	f	j/f
		1	10.6	4.81	57	.0054	0.0163	.330
		2	15.5	4.73	95	.0061	0.0144	.424
		3	22.3	4.62	111	.0050	0.0123	.407
		4	29.4	4.59	131	.0045	0.0117	.381
0.063 in.	3.95	5	38.8	4.67	183	.0047	0.0108	.434
		6	49.2	4.70	206	.0042	0.0100	.420
		7	67.8	4.70	254	.0037	0.0099	.378
		8	90.5	4.75	327	.0036	0.0098	.369
		1	6.12	4.73	67	.0111	0.0675	.165
		2	9.45	4.56	96	.0102	0.0611	.165
		3	14.20	4.47	120	.0084	0.0578	.146
		4	18.90	4.41	150	.0079	0.0547	.145
0.072 in.	1.12	5	25.3	4.48	181	.0072	0.0506	.142
		6	32.4	4.47	224	.0069	0.0474	.145
		7	41.2	4.43	282	.0068	0.0458	.149
		8	48.8	4.32	312	.0064	0.0466	.137
		1	9.6	4.68	93	.0097	0.0551	.176
		2	14.7	4.63	121	.0082	0.0498	.167
		3	20.7	4.58	147	.0071	0.0436	.163
		4	28.5	4.48	187	.0066	0.0408	.161
0.072 in.	1.65	5	42.8	4.48	250	.0059	0.0365	.160
		6	48.8	4.41	270	.0055	0.0342	.161
		7	59.5	4.35	320	.0054	0.0350	.154

.... Cont'd ....

APPENDIX E

DERIVED RESULTS

Wire Size	H/D Ratio	Test	Re x 10^{-3}	Pr	$Nu/Pr^{1/3}$	j	f	j/f
		1	10.1	4.73	62	.0061	0.0356	.172
		2	14.9	4.59	82	.0055	0.0260	.212
		3	22.3	4.52	110	.0049	0.0176	.280
		4	39.4	4.52	177	.0045	0.0127	.354
0.072 in.	2.95	5	48.0	4.48	205	.0043	0.0119	.359
		6	65.8	4.46	273	.0041	0.0118	.352
		7	76.5	4.36	295	.0039	0.0115	.336
		8	89.5	4.31	316	.0035	0.0121	.292
		9	103.7	4.15	420	.0041	0.0119	.340
		1	10.4	4.73	52	.0050	0.0359	.140
		2	15.7	4.64	76	.0049	0.0274	.178
		3	22.3	4.47	96	.0043	0.0191	.225
		4	31.2	4.36	137	.0044	0.0139	.317
0.072 in.	3.94	5	46.7	4.39	180	.0039	0.0105	.367
		6	60.3	4.37	214	.0035	0.0099	.358
		7	74.6	4.28	266	.0036	0.0096	.372
		8	90.0	4.22	306	.0034	0.0092	.370
		9	107.0	4.07	346	.0032	0.0090	.360
		1	10.0	4.84	51	.0051	0.0389	.131
		2	15.3	4.68	69	.0045	0.0253	.177
		3	21.9	4.63	98	.0045	0.0168	.267
		4	31.0	4.37	127	.0041	0.0118	.347
0.072 in.	5.50	5	45.7	4.39	178	.0039	0.0092	.425
		6	60.5	4.39	227	.0037	0.0085	.442
		7	80.4	4.33	282	.0035	0.0081	.433
		8	95.5	4.20	331	.0035	0.0079	.438
		9	102.0	4.14	346	.0034	0.0077	.440

... Cont'd ...

APPENDIX E

DERIVED RESULTS

Wire Size	H/D Ratio	Test	Re x 10^{-3}	Pr	$Nu/Pr^{1/3}$	j	f	j/f
		1	9.7	5.01	66	.0068	0.0203	.337
		2	14.4	4.66	79	.0055	0.0173	.317
		3	22.6	4.61	113	.0050	0.0151	.331
		4	38.3	4.68	181	.0047	0.0135	.350
0.072 in.	2.95	5	46.5	4.68	210	.0045	0.0123	.366
		6	63.8	4.78	285	.0045	0.0123	.363
	(Rerun)							
		1	10.2	4.97	58	.0057	0.0177	.322
		2	15.3	4.68	84	.0055	0.0143	.386
		3	21.4	4.56	110	.0051	0.0119	.430
0.072 in.	3.94	4	29.6	4.59	131	.0044	0.0108	.410
	(Rerun)	5	37.4	4.70	170	.0045	0.0104	.435
		6	50.7	4.78	212	.0042	0.0099	.423
		7	70.3	4.86	253	.0036	0.0094	.382
		8	92.5	4.68	309	.0033	0.0094	.355
		1	10.0	4.97	53	.0053	0.0150	.356
		2	13.1	4.64	72	.0055	0.0131	.418
		3	19.2	4.73	102	.0053	0.0105	.508
		4	23.4	4.73	116	.0050	0.0100	.495
0.072 in.	5.50	5	34.7	4.84	151	.0044	0.0095	.458
	(Rerun)	6	47.1	5.00	192	.0041	0.0085	.478
		7	66.0	4.84	250	.0038	0.0081	.466
		8	86.4	4.76	311	.0036	0.0080	.450

.... Cont'd ....

APPENDIX E

DERIVED RESULTS

Wire Size	H/D Ratio	Test	Re x 10^{-3}	Pr	$Nu/Pr^{1/3}$	j	f	j/f
		1	12.5	4.53	44	.00351	0.0113	.315
		2	17.8	4.33	62	.00346	0.0074	.468
		3	27.5	4.41	80	.00288	0.0053	.545
		4	46.0	4.64	137	.00292	0.0051	.572
Empty Tube		5	56.0	4.53	150	.00268	0.0053	.506
		6	81.5	4.44	208	.00255	0.0048	.531
		7	98.5	4.33	237	.00240	0.0046	.522
		8	121.0	4.15	289	.00230	0.0045	.530
		9	137.0	4.15	363	.00265	0.0050	.530

APPENDIX F

Analysis of Heat Losses and Temperature Drop

a) Conduction Along Tube:

In order to evaluate the heat transferred away from the heated length by conduction in the tube wall, a fin analysis was performed.

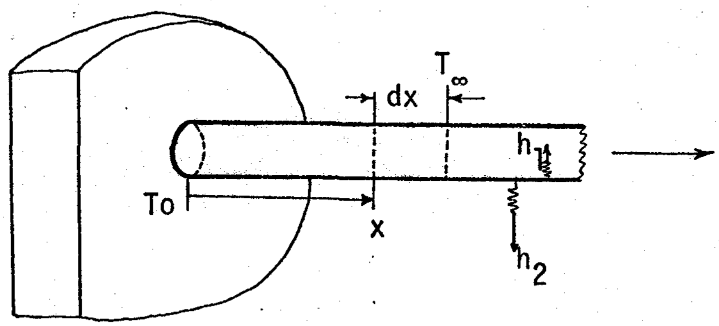

FIGURE 21

Assuming

(1) The temperature of the copper lug to be the same as that of the tube

(2) The temperature of water entering the test section or leaving the test section is the same and equal to the temperature of the ambient air outside the test section.

D.E.

$$\frac{d}{dx}\left(KA\frac{d\Theta}{dx}\right) - \Theta(h_1P_1 + h_2P_2) = 0$$

where

$\Theta = (T - T_\infty)$

A = Crossectional area of tube

P = Perimeter of tube

h_1 = Inside film heat transfer coefficient

h_2 = Outside film heat transfer coefficient.

B.C.

$$T \text{ at } x = 0 = To$$

so that $$\Theta(0) = \Theta_0$$

$$\frac{d\Theta}{dx}(\infty) = 0$$

D.E.

$$\frac{d^2\Theta}{dx^2} - m^2\Theta = 0 \qquad (1)$$

where $$m^2 = \frac{h_1P_1 + h_2P_2}{KA}$$

B.C.

$$\Theta(0) = \Theta_0 \qquad (2)$$

$$\frac{d\Theta(0)}{dx} = 0 \qquad (3)$$

The solution to the D.E. (1) for the B.C. (2) and B.C. (3) is given in Kreith (11).

$$\frac{\Theta}{\Theta_0} = \frac{\text{Cosh } m(L - x)}{\text{Cosh } (mL)} \qquad (4)$$

which is further solved to give

$$q = (h_1P_1 + h_2P_2)K \quad A \quad \tanh (mL) \qquad (5)$$

For the present configuration

$$h_1 = 5000 \ \frac{BTU}{hr.\ Ft^2.\ °F}$$

$$h_2 = 1.0 \ \frac{BTU}{hr.\ Ft^2.\ °F}$$

$h_1 >> h_2$ and therefore h_2 can be neglected.

$$P_1 = 2\pi r_i = 2\pi \times \frac{0.24}{12} \text{ Ft.} = 0.126 \text{ Ft.}$$

$$K = 8.6 \frac{\text{BTU}}{\text{hr. Ft. °F}}$$

$$A = \pi (r_2^2 - r_1^2)$$

$$= \frac{\pi}{144} (0.25^2 - 0.24^2)$$

$$= .107 \times 10^{-3} \text{ Ft}^2$$

$$m^2 = \frac{h_1 P_1 + h_2 P_2}{KA} = \frac{h_1 P_1}{KA}$$

$$= \frac{5000 \times .126}{8.6 \times .107 \times 10^{-3}} = 827$$

$$L = 5''$$

$$q = h_1 P_1 K \ A \ \tanh (mL)$$

$$= 5000 \times .126 \times 8.6 \times .107 \times 10^{-3} \ \tanh(\infty)$$

$$= .761 \ \frac{\text{BTU}}{\text{hr}}$$

This amount of heat loss is negligible in comparison with the minimum rate of heat generation in the heated length.

b) <u>Temperature Drop in The Wall</u>:

In order to evaluate the temperature drop in the tube wall a steady state conduction analysis for the heater tube was performed.

$$\frac{d^2T}{dr^2} + \frac{1}{r} \frac{dT}{dr} + \frac{Q'''}{K} = 0$$

is Poisson's Equation in cylindrical coordinates for steady state heat conduction in a solid with homogeneous internal heat generation.

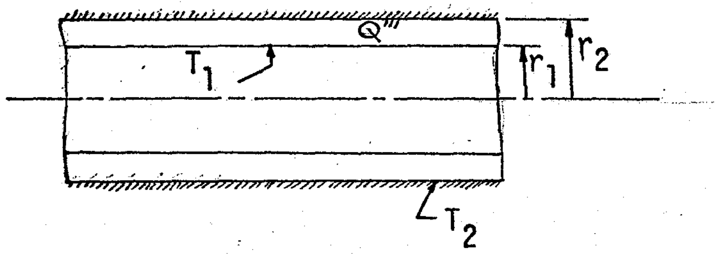

FIGURE 22

B.C.

$$T(r_2) = T_2$$

$$T(r_1) = T_1$$

And assuming adiabatic outer surface

$$\frac{dT}{dr}(r_2) = 0$$

This equation with the above mentioned boundary conditions is solved in Appendix (2.1) of Reference (7) to give

$$T_i - T_o = \frac{Q'''}{2K}(r_2^2 - r_1^2)\left[\frac{1}{2} - \frac{r_2^2}{r_2^2 - r_1^2}\ln\frac{r_2}{r_1}\right]$$

In the present case

$$Q''' = \frac{Q_{Max}}{Volume}$$

$$Q_{Max} = 45{,}000\ \frac{BTU}{hr.}$$

$$Volume = \pi(r_2^2 - r_1^2) \times L$$

$$= \frac{\pi}{144}(.25^2 - .24^2) \times 2\ Ft^3 = 0.214 \times 10^{-3} Ft^3$$

$$Q''' = \frac{45,000}{.214 \times 10^{-3}} = 210 \times 10^{6} \frac{BTU}{Hr.Ft^{3}}$$

$$K = 8.6 \frac{BTU}{hr.Ft.°F}$$

$$(T_i - T_o) = \frac{210 \times 10^6}{8.6} \times \frac{(.25^2 - .24^2)}{144} \left[0.5 - \frac{0.25^2}{(.25^2 - .24^2)} \ln \frac{0.25}{0.24} \right] = -9°F$$

This value is quite significant. Consequently, while making calculations for the inside film heat transfer coefficient this temperature drop was subtracted from the measured values of ΔT_f and T_f.

c) Heat Loss Through Insulation:

In order to evaluate the heat loss through the lagging, a steady state conduction analysis was performed for the one inch thick insulation layer. Assuming the end effects negligible and the inner surface temperature of the insulation constant, the rate of heat conduction through insulation is,

$$q_{ins.} = -KA \frac{dT}{dr}$$

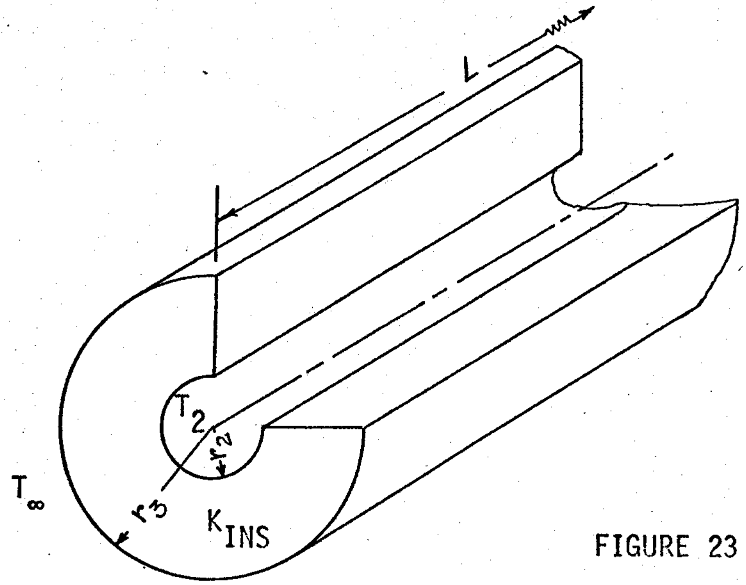

FIGURE 23

The solution is obtained in Chapter (2.1) of Reference (11).

$$q_{ins.} = \frac{T_2 - T_\infty}{\ln\left(\frac{r_3}{r_2}\right)} \Big/ 2\pi\, K_{ins.} L$$

where r_3 = Outside diameter of insulation = $\frac{1.5}{12}$ Ft.

r_2 = Inside diameter of insulation = $\frac{0.5}{12}$ Ft.

T_2 = 130°F

T_∞ = 75°F

$K_{ins.} = 0.022 \dfrac{\text{BTU}}{\text{hr. Ft. °F}}$

L = 2 Ft.

$$q_{ins.} = \frac{(130 - 75)}{\ln \frac{1.5}{.5}\,(2\pi \times .022 \times 2)}$$

$$= 14 \text{ BTU/hr.}$$

This amount of heat loss is negligible in comparison with the minimum rate of heat generation in the tube.